antioxidants

MDPI

Review

Selenium-Containing Biomaterials for Musculoskeletal Disease Therapy: From Fabrication to Mechanistic Insights and Clinical Translation

Yitian Sun [1,2], Xue Ding [1,2,3], Yi Yang [4], Fan He [1,2,*] and Xi Chen [5,*]

[1] Orthopaedic Institute, Suzhou Medical College, Soochow University, Suzhou 215006, China; 2430805044@stu.suda.edu.cn (Y.S.); 20244250003@stu.suda.edu.cn (X.D.)
[2] Department of Orthopaedics, The First Affiliated Hospital of Soochow University, Soochow University, Suzhou 215006, China
[3] School of Life Science, Suzhou Medical College, Soochow University, Suzhou 215006, China
[4] The Second Affiliated Hospital of Soochow University, Soochow University, Suzhou 215006, China; yyfedu@126.com
[5] Department of Pathology, The Third Affiliated Hospital of Soochow University, Changzhou 213003, China
* Correspondence: fanhe@suda.edu.cn (F.H.); chenxi1124@suda.edu.cn (X.C.); Tel.: +86-512-6778-1420 (F.H.); +86-519-6887-0891 (X.C.)

Abstract

The escalating prevalence of musculoskeletal diseases (MSDs) is associated with global population aging. Selenium (Se)-containing biomaterials have currently attracted increasing attention for treating these conditions. In organisms, exogenous or endogenous selenium can be metabolized and co-translationally incorporated into selenoproteins in the form of selenocysteine (Sec), including glutathione peroxidases (GPXs, such as Sec-containing GPX1-4 and GPX6), thioredoxin reductases (TXNRDs), and iodothyronine deiodinases (DIOs). These selenoproteins help maintain redox homeostasis, inhibit ferroptosis, and regulate immune responses. Meanwhile, selenium-containing biomaterials can exert multifaceted therapeutic effects through their intrinsic GPX-mimicking nanozyme catalytic activity, diselenide bond-mediated redox-responsive drug release, and associated signaling pathway regulation. Herein, we provide a comprehensive overview of recent advances in the fabrication, physicochemical properties, cellular signaling modulation, and preclinical therapeutic applications of Se-containing biomaterials. We systematically examine various fabrication platforms ranging from inorganic and organic systems to composite matrices and nanoparticles. Then we highlight how their physicochemical properties dictate Se release kinetics and degradation profiles. We further discuss the underlying mechanisms by which these dynamic scaffolds modulate cellular microenvironments, specifically focusing on macrophage immunometabolism, antibacterial efficacy, and the lineage-specific differentiation of musculoskeletal cells. Based on distinguishing the intrinsic catalytic activity of materials, endogenous selenoprotein-dependent responses, related signaling pathway changes, and accompanying carrier component effects, this article systematically evaluates their applications in preclinical models of osteoporosis, osteoarthritis, intervertebral disc degeneration, and skeletal muscle diseases. It connects materials design with selenium biology, providing a conceptual framework and reference for the rational design of future regenerative therapies.

Keywords: selenium-containing biomaterials; selenoproteins; musculoskeletal diseases; redox homeostasis; tissue regeneration; microenvironment modulation

Academic Editor: William T. Self

Received: 25 September 2026
Revised: 25 October 2026
Accepted: 27 October 2026
Published: 24 November 2026

Copyright: © 2026 by the authors. Licensee MDPI, Basel, Switzerland. This article is an open access article distributed under the terms and conditions of the Creative Commons Attribution (CC BY) license.

1. Introduction

Selenium (Se) is an essential trace element that helps maintain systemic homeostasis [1]. Unlike major elements, Se acts mainly by being inserted into proteins as selenocysteine (Sec), where it forms the catalytic center rather than simply activating the enzyme [2]. So far, 25 different selenoproteins have been identified in the human genome. Among these, the glutathione peroxidase (GPX), thioredoxin reductase (TXNRD), and iodothyronine deiodinase (DIO) families are the most thoroughly studied [3]. In the musculoskeletal system, this protein network creates a basic defense mechanism. It clears out oxidative stress, controls inflammatory cascades, and keeps the cellular redox environment stable. Se also helps metabolize thyroid hormones, an indirect pathway that strongly affects bone remodeling and overall metabolic balance [4].

The physiological functions of musculoskeletal tissues depend closely on Se-dependent metabolic mechanisms. Clinical observations consistently show that adequate Se status correlates with healthy muscle mass and strength. A lack of Se, on the other hand, frequently links to myopathy and abnormal bone growth. A cross-sectional epidemiological study of 2983 U.S. adults (NHANES 2013–2014) supported this observational association: higher serum selenium levels were independently associated with higher femoral bone mineral density (BMD), lower Fracture Risk Assessment Tool (FRAX) 10-year fracture risk estimates, and lower self-reported history of prior fractures. However, such cross-sectional associations cannot directly establish a causal protective effect [5]. In terms of pathology, severe environmental Se shortage acts as a known primary cause for Kashin-Beck disease (KBD), an endemic joint disorder. Without enough Se, the catalytic function of GPXs and TXNRDs fails, leading to unchecked oxidative stress and subsequent chondrocyte death. This process eventually ruins the turnover of the cartilage extracellular matrix (ECM) and leaves patients with irreversible skeletal deformities. The effects of a systemic Se deficiency also reach beyond orthopedics. Studies show it can worsen vascular endothelial dysfunction, speed up myocardial injury, harm neural network growth, and delay normal skin healing [6–9].

Biomaterials such as bone grafts, synthetic scaffolds, and metallic implants are commonly used in orthopedics to provide mechanical support and facilitate tissue regeneration [10]. However, a major flaw of standard implants is that they are mostly biologically inert. They lack the built-in ability to ease the excessive oxidative stress and inflammation found in diseased or injured joints. Adding Se into tissue-engineered scaffolds has become a practical way to close this treatment gap [11]. Embedding Se into hydrogels, bioceramics, or polymer composites allows for a steady, localized release of therapeutic ions. Releasing these ions in a controlled way changes the injury environment. It traps reactive oxygen species (ROS) and pushes macrophages to adopt anti-inflammatory traits, setting up favorable conditions for faster tissue repair [12]. Surfaces modified with Se have also been shown to help progenitor cells attach and differentiate properly, while protecting new tissue from sudden oxidative damage [13]. At the same time, these modified materials carry natural broad-spectrum antibacterial properties, which could significantly cut down the rate of implant-associated infections [14]. These advantages lead to favorable repair results in different orthopedic applications (Figure 1).

As a narrative review bridging materials engineering and selenoprotein biology, this article systematically searched PubMed, Web of Science, and Scopus for relevant English-language literature published up to early 2026. Core search terms included combinations of “selenium”, “selenoprotein”, “selenium nanoparticles”, “selenite”, “diselenide”, “biomaterials”, “hydrogel”, “scaffold” with “bone”, “osteoporosis”, “osteoarthritis”, “cartilage”, “intervertebral disc”, “skeletal muscle”, “sarcopenia”, “macrophage”, and “ferroptosis.” Literature inclusion followed a three-tier complementary logic: (1) Core evidence

tier focused on experimental studies evaluating the physicochemical properties and therapeutic efficacy of selenium-containing biomaterials (covering inorganic selenium, zero-valent nanoselenium, organic selenium, and composite scaffolds) in in vitro and in vivo models of bone, cartilage, intervertebral disc, and skeletal muscle diseases; (2) Mechanistic background tier selectively included basic biology studies using genetic knockout/knockdown (e.g., Gpx1, Selenow, Sephs1, Terc) or biochemical approaches to elucidate the mechanisms of endogenous selenoproteins in musculoskeletal cells; (3) Clinical relevance tier included representative population-based epidemiological observations and whole-body nutritional intervention studies to provide disease context and comparison with local biomaterial delivery strategies. Throughout the review, we paid particular attention to distinguishing different evidence levels (epidemiological association, whole-body nutritional supplementation, and local biomaterial intervention) and different mechanisms of action (material-intrinsic nanozyme catalysis, endogenous selenoprotein-dependent regulation, and accompanying carrier effects) to ensure the accuracy of scientific interpretation.

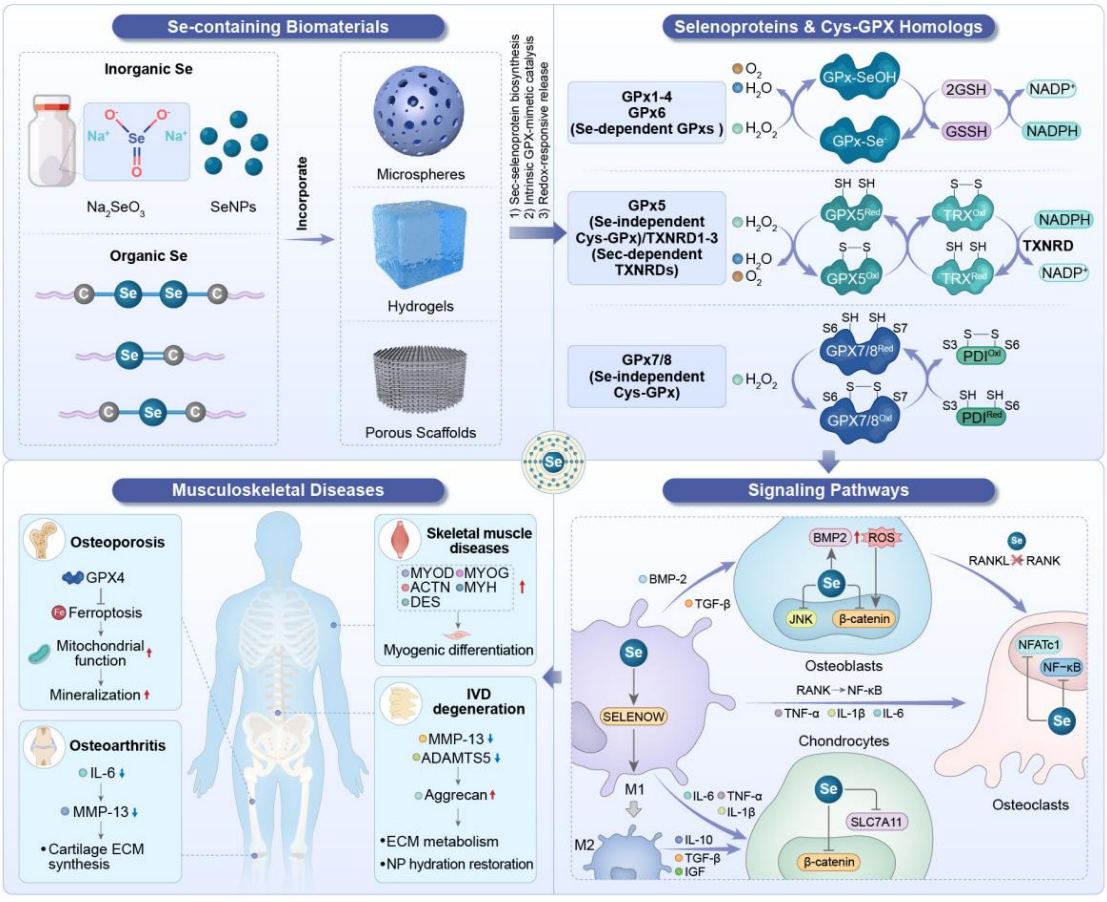

Figure 1. Conceptual framework of selenium-containing biomaterials in musculoskeletal diseases. Inorganic, elemental nano-selenium, and organic selenium platforms modulate the pathological microenvironment through three distinct modes of action: (1) supplying bioavailable selenium precursors to support endogenous Sec-containing selenoprotein (e.g., GPX1-4, GPX6, TXNRD1-3, and DIO1-3) biosynthesis and activity, while distinguishing them from Se-independent Cys-containing GPX homologs (GPX5, GPX7, and GPX8); (2) exerting material-intrinsic GPX-mimicking nanozyme catalysis; and (3) enabling redox-responsive drug release via dynamic diselenide bonds, collectively regulating downstream signaling pathways and cellular differentiation across musculoskeletal tissues.

2. Diverse Physiological Functions of Selenoproteins

Selenoproteins are defined by the presence of Sec and these proteins are expressed in the thyroid, liver, kidneys, brain, and immune cells. In these areas, selenoproteins control antioxidant defense, regulate metabolism, and manage immune functions [3]. Their main physiological role is to remove excess ROS and maintain redox equilibrium [15]. At physiological levels, ROS participate in signaling and metabolism; however, excessive ROSs caused by external stress or metabolic dysfunction result in oxidative stress. This damages proteins, nucleic acids, and lipids, leading to apoptosis, chronic inflammation, and tissue degeneration [16]. Selenoproteins are the primary defense against such oxidative damage and help preserve tissue integrity by regulating calcium flux, endoplasmic reticulum proteostasis, and signal transduction to support cellular metabolism and function [17]. The tissue distribution and functions of major selenoproteins are listed in Table 1.

Table 1. Classification, structural characteristics, and physiological functions of major Sec-containing selenoproteins and Se-independent Cys-containing GPX homologs.

Family	Type	Active Site	Structure	Expression Sites	Unique Feature	References
Se-dependent GPXs (Sec-containing): GPX1–4, GPX6						
GPX	GPX1	Sec	Tetramer	Cytoplasm, Mitochondria	Most universally expressed	[18,19]
	GPX2	Sec	Tetramer	Gastrointestinal tract	Intestinal specific	[20]
	GPX3	Sec	Tetramer	Kidney, Plasma	Only secreted form	[21]
	GPX4	Sec	Monomer	Testes, Ubiquitous	Unique direct reducer of phospholipid hydroperoxides	[22]
	GPX6	Sec	Tetramer	Olfactory organs	Significant species differences	[18]
Se-independent GPX homologs (Cys-containing, non-selenoproteins): GPX5, GPX7, GPX8						
	GPX5	Cys	Tetramer	Epididymis	Associated with sperm maturation	[18,23]
	GPX7	Cys	Monomer	Endoplasmic reticulum	ER-resident	[18,23]
	GPX8	Cys	Monomer	Endoplasmic reticulum	Involved in calcium signaling and ER stress	[18,23]
TXNRD	TXNRD1	Sec	Homodimer	Cytoplasm	Major housekeeping selenoenzyme	[24]
	TXNRD2	Sec	Homodimer	Mitochondria	Essential for mitochondrial redox regulation	[25]
	TXNRD3	Sec	Homodimer	Testis	Dual TXNRD and Grx activity	[26]
DIO	DIO1	Sec	Homodimer	Liver, Kidney, Thyroid	Activates T4 to T3, inactivates rT3 to T2	[27,28]
	DIO2	Sec	Homodimer	Brain, Pituitary	Tissue-specific T3 producer, neurodevelopment and thermogenesis	[28]
	DIO3	Sec	Homodimer	Placenta, Fetal tissues	Fetal protector, sole inactivator	[27]

2.1. The GPX Family

The GPX protein family reduces oxidative damage by using glutathione (GSH) as an electron donor. This process breaks down hydrogen peroxide (H_2O_2) and hydroperoxides. Scavenging these chemicals early stops highly destructive hydroxyl radicals from forming and protects cellular macromolecules from severe oxidative injury [18].

The GPX family contains eight different isoforms. They are distributed in different tissues and target different substrates, and their antioxidant ability relies on steady renewal of their catalytic center. These isoforms fall into two groups based on how they

work: Se-dependent and Se-independent. The Se-dependent members (GPX1–4 and GPX6) have a reactive Sec residue at their catalytic center. During the peroxide reduction step, this Sec temporarily oxidizes into selenenic acid (Sec-SeOH). A continuous cycle then restores the Sec back to its active state. This cycle is powered by GSH and the enzyme glutathione reductase (GR). Inside this group, each isoform targets a distinct biological area. GPX1 exists in the cytosol and mitochondria of skeletal muscle and bone cells [19]. GPX2 is mostly found in the gut lining and helps keep the mucosal barrier intact [20]. GPX3 is released into blood plasma and extracellular fluids to provide whole-body antioxidant defense [21]. GPX4 is the only isoform that breaks down phospholipid hydroperoxides in cell membranes. It is a key blocker of ferroptosis and is vital for muscle cell survival and skeletal health [22].

The Se-independent isoforms (GPX5, GPX7, and GPX8) replace Sec with a standard cysteine residue, so they do not rely on the classic GSH cycle. Instead, these enzymes use alternative thiol-based networks that involve protein thiols or protein disulfide isomerase (PDI) [18]. In terms of function, they control very specific local tasks. These tasks include helping epididymal sperm mature, handling olfactory signaling, and supporting oxidative protein folding inside the ER [23].

2.2. The TXNRD Family

The TXNRD protein family includes three Se-containing flavoproteins: TXNRD1 in the cytosol, TXNRD2 in mitochondria, and TXNRD3 specific to the testes. These enzymes fight oxidative stress mainly through the thioredoxin (TXN)-peroxiredoxin (PRDX) axis. The process involves moving electrons from NADPH through a flavin adenine dinucleotide (FAD) domain. The electrons go directly to the Sec active site of the TXNRD enzyme. The enzyme then reduces oxidized TXN to help clear out ROS via PRDX. Even when local TXN levels drop, the highly reactive Sec residue can still directly neutralize oxidative stress using secondary pathways.

TXNRD1 is mostly found in the cytoplasm and keeps cellular redox balance steady. When thioredoxin-interacting protein (TXNIP) blocks TXNRD1, redox balance is disrupted and GPX4-driven ferroptosis is triggered. In rat models of type 2 diabetic osteoporosis, this damages trabecular bone structure and lowers BMD [24]. TXNRD2 only exists in mitochondria. It helps keep these organelles stable and supports oxidative phosphorylation, which provides energy for high-demand tasks like matrix synthesis [25]. TXNRD3 is nearly exclusive to the testes. It maintains redox balance and mitochondrial function in sperm-producing cells, and supports sperm development and male reproductive function [26].

2.3. The DIO Family

The iodothyronine deiodinase (DIO) family includes DIO1, DIO2, and DIO3. All three depend entirely on Sec to function. They control the activation and deactivation of thyroid hormones through a process called reductive deiodination. DIO1 and DIO2 manage outer-ring deiodination. This chemical reaction converts the prohormone thyroxine (T4) directly into biologically active triiodothyronine (T3). DIO3 works in the opposite direction. It uses inner-ring deiodination to break down both T4 and T3 into their inactive forms, reverse T3 (rT3) and T2. Cells need to adapt quickly to changing physiological conditions, like tissue hypoxia or thyroid dysfunction. To achieve this, they rapidly adjust their local DIO activity. They make these adjustments at the transcriptional level and through fast ubiquitin-proteasome degradation pathways [27].

The specific locations of these enzymes determine their biological roles. DIO1 anchors mostly to the plasma membranes in the liver, kidneys, and thyroid gland. It acts like a systemic regulator that clears out rT3 and keeps circulating T3 levels steady. A strict

feedback loop involving Se availability and thyroid hormone status controls its expression. A drop in DIO1 activity serves as a classic clinical sign of low T3 syndrome [28]. The ER-resident DIO2 does a different job. It generates intracellular T3 locally for tissues that consume large amounts of oxygen, such as the brain, brown adipose tissue, and skeletal muscle. By providing local T3, DIO2 acts as a main driver for neuronal myelination and heat generation. If DIO2 levels fall too low, the deficiency severely damages auditory development and breaks the neuroendocrine loop that regulates pituitary TSH secretion [28]. Finally, plasma membrane-bound DIO3 acts as a physiological brake to dampen excessive hormone signals. Fetal and placental tissues express it in high amounts. Adult tissues can also reactivate DIO3 expression when hit by sudden hypoxic or inflammatory events. Once active again, it participates in local wound healing processes and strongly influences tumor progression.

3. Preparation and Characterization of Se-Containing Biomaterials

3.1. Biomaterials Incorporating Sodium Selenite

Sodium selenite (Na_2SeO_3) has an ionic crystal structure and acts as a bioactive ion. It exists mainly as anhydrous or pentahydrate forms and dissolves well in water, rapidly releasing selenite anions and making it an efficient Se donor for hydrogels, microspheres, and other platforms [29]. It has only moderate heat stability, so it must be processed carefully to avoid breaking down into oxides. But its release rate can be adjusted by changing the porosity and crosslink density of the carrier to fit tissue repair timelines. Na_2SeO_3 has different biological effects at different concentrations: low doses support antioxidant enzyme production and tissue regeneration, while high doses can be toxic to cells [30]. Researchers have incorporated Na_2SeO_3 into various biomaterials by blending, in situ precipitation, and electrospinning. For example, Ressler et al. combined Na_2SeO_3 with cuttlefish bone-derived calcium carbonate by wet precipitation to produce selenite-substituted calcium phosphate with improved thermal stability and bioactivity [31].

3.2. Biomaterials Incorporating Selenium Nanoparticles (SeNPs)

SeNPs are zero-dimensional nanomaterials made of zero-valent Se aggregates, typically 1–100 nm in diameter. Compared with inorganic Se precursors, they show better biocompatibility and lower acute toxicity because intracellular thiols gradually reduce them to bioavailable selenide ions for selenoprotein synthesis [32]. At therapeutic concentrations they are generally safe, but toxicity is size-dependent: very small particles have high surface energy and can be cytotoxic despite enhanced bioavailability [33]. SeNPs exert their effects mainly through selenol groups that neutralize ROS, giving them antioxidant properties [34]. They have poor aqueous solubility and can oxidatively dissolve under acidic or environmental stress, but surface functionalization with organic ligands stabilizes them. The high density of coordinatively unsaturated Se atoms allows coordination or covalent bonding with sulfur- and nitrogen-containing groups, enabling the design of stable, bioactive nanosystems [35].

Chemical reduction is the most common method for making SeNPs. Na_2SeO_3 is often chosen as the Se source because of its good solubility, moderate reactivity, and low cost. Mild reducing agents are preferred because they provide gentle reaction kinetics and often have antioxidant properties that help prevent agglomeration [36].

Physical methods avoid chemical reducing agents and use energy input to drive phase transformation and nucleation. They produce high-purity products with well-defined morphology. In pulsed laser ablation, for example, a high-purity Se target is vaporized into a plasma that condenses into nanoparticles in liquid (Figure 2A) [37]. Ultrasonic cavitation and gamma-ray irradiation also use harsh physical conditions to break down

precursors or produce solvated electrons for reduction. They are usually paired with natural stabilizers like chitosan or plant extracts to enhance biocompatibility [38]. Because of their high purity and lack of chemical residues, physically synthesized SeNPs are suitable for applications such as antitumor vectors, antibacterial coatings, drug delivery systems, and biofunctionalized implant surfaces.

Pushing beyond conventional reduction paradigms, Ishtiaq et al. used chemical bath deposition instead of conventional reduction to synthesize SeNPs. Elemental selenium was refluxed with sodium sulfite to make a precursor solution, which was then reacted in an ammoniacal bath where fluorine-doped tin oxide substrates controlled the deposition of nanostructured selenium (Figure 2B) [39]. To address the persistent challenges of industrial scalability and long-term stability, He et al. developed a confined coordination reduction strategy using lentinan polysaccharide matrices. Hydrogen bonding and van der Waals forces within the biopolymer network restrict the reduction process, suppressing agglomeration and unwanted crystalline phase transitions for long-term storage stability [40].

Biosynthetic methods use natural biomolecules from living systems for reduction and capping, prioritizing sustainability and biocompatibility. Illustrating this principle, Huang et al. isolated *Acinetobacter sp. SX5* from Se-rich soil and used its enzymes to reduce Na_2SeO_3 into spherical SeNPs stabilized by surface-adsorbed biomacromolecules, with high colloidal stability and conversion efficiency (Figure 2C) [41]. More recent approaches use cell-free systems with biomolecules secreted by microorganisms, avoiding the need to maintain viable cells. For instance, Kim et al. used the cell-free supernatant of *Lactiplantibacillus plantarum* cultures to reduce Na_2SeO_3 and generate stable SeNPs (Figure 2D) [42].

3.3. Organic Se-Based Biomaterials

3.3.1. Selenoether

Organic Se-containing biomaterials use organic Se moieties to provide antioxidant, anti-inflammatory, and pro-regenerative effects. Selenoether structures have stable Se–C single bonds and are suitable for long-term implants and scaffolds that need high structural integrity. Capitalizing on this durability, Tian et al. built a metal-free nanozyme by integrating antioxidant enzymes into a Se-containing hydrogen-bonded organic framework, then added targeting peptides to improve biocompatibility and stability [43].

3.3.2. Diselenide

Diselenide-bridged biomaterials contain dynamic Se–Se covalent bonds that are redox-reversible, making them useful for responsive drug delivery and biodegradable hydrogels. Exploiting this responsive nature, Yu et al. synthesized mesoporous silica nanoparticles cross-linked with diselenide bonds and loaded them with leucine, achieving good biodegradability and a high specific surface area for improved therapeutic safety [44].

Diselenide bonds (–Se–Se–) bridge chemical engineering and biomedical regulation. Compared to disulfide bonds, they have lower bond energy, longer bond length, and stronger nucleophilicity. These features make them environmentally responsive, capable of dynamic exchange, and able to self-heal under mild physiological conditions. High levels of ROS break diselenide bonds, allowing drugs to be released in a controlled way at lesion sites. The released Se can trigger the NRF2-mediated antioxidant pathway. Translating this dual functionality into OA therapy, Li et al. synthesized HO–SeSe–OH and then covalently linked two diclofenac molecules to both ends of the diselenide bond by condensation, producing the amphiphilic prodrug DSeD. The diselenide bond serves as both a chemical linker and an ROS-responsive cleavage site. This material achieves targeted

drug release and multimodal OA therapy combining anti-inflammatory analgesia, antioxidant defense, and cartilage repair [45].

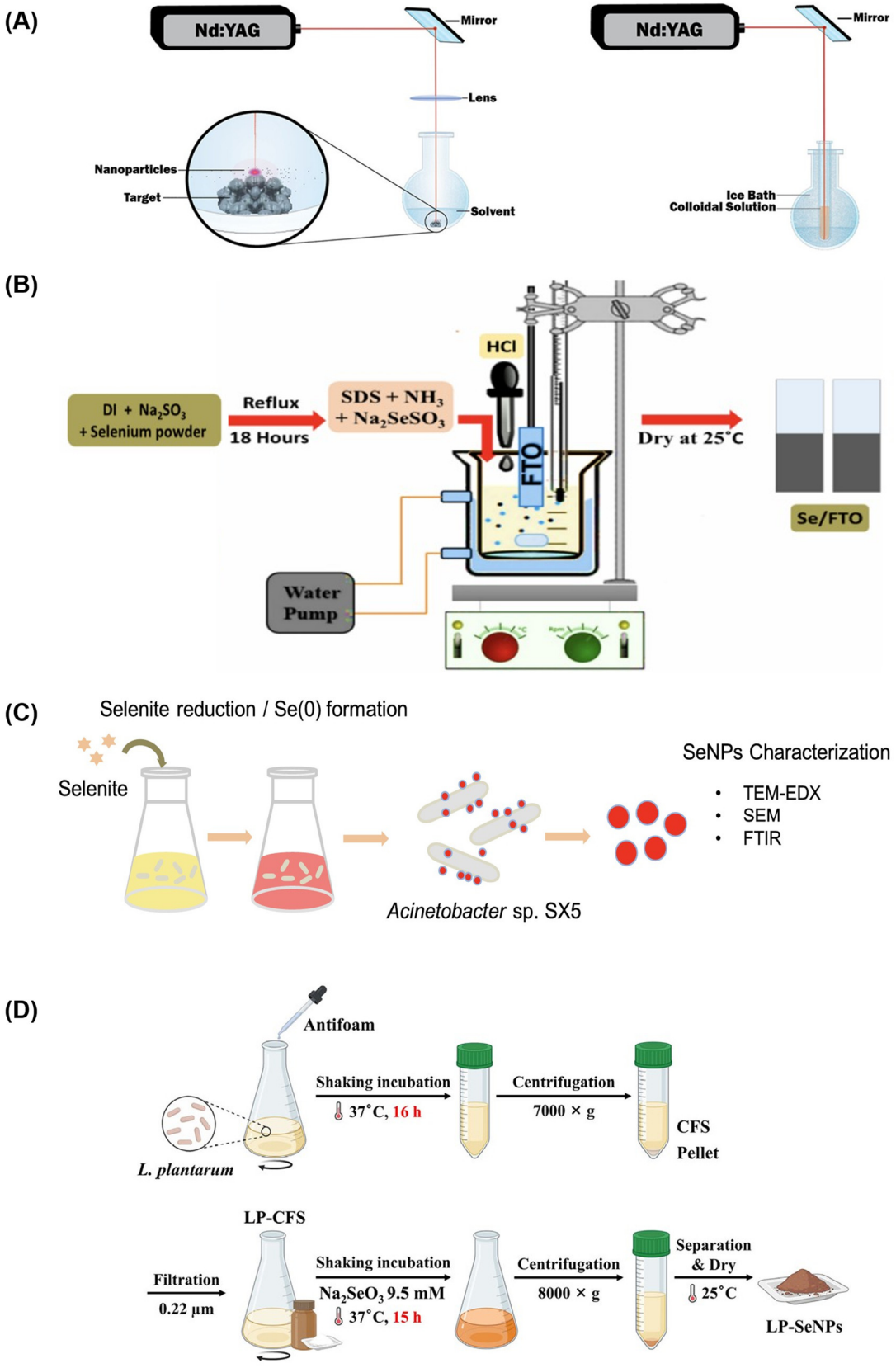

Figure 2. Preparation methods for SeNPs: chemical, physical, and biological methods. (**A**) SeNPs were synthesized by liquid-phase laser ablation. Adapted from Ref. [37] under the terms of the Cre-

ative Commons Attribution License (CC BY). (**B**) SeNPs were synthesized by chemical bath deposition. Adapted from Ref. [39] under the terms of the Creative Commons Attribution License (CC BY). (**C**) Process of preparing SeNPs by reducing selenite using *Acinetobacter sp. SX5*. Reprinted with permission from Ref. [41]. License Number: 6311660060644. Copyright 2025, Elsevier. (**D**) Schematic representation of SeNPs synthesis using LP-CFS. Adapted from Ref. [42] under the terms of the Creative Commons Attribution License (CC BY).

3.3.3. Selenourea

Selenourea derivatives contain characteristic functional groups with strong hydrogen bond donor/acceptor capabilities and radical scavenging activity. Moussa et al. synthesized a series of novel aryl, benzyl, and piperazinyl small-molecule selenourea derivatives under mild room-temperature conditions, performed systematic structural characterization, and demonstrated in vitro their significant DPPH radical scavenging ability, broad-spectrum antibacterial activity, and anti-cancer cell proliferation effects [46]. Although current research on selenoureas mainly focuses on small-molecule synthesis and in vitro pharmacological evaluation, given that urea/selenourea groups can form intermolecular hydrogen bond networks, they are expected to be introduced as supramolecular crosslinking motifs into hydrogels or coating systems in the future to explore their application potential in orthopedic soft/hard tissue interface repair.

3.4. Selenium-Doped Inorganic Bioceramics/Bioactive Glasses and Inorganic-Organic Composite Biomaterials

To overcome the limitations of a single free selenium precursor or bare selenium nanoparticles, such as burst release, agglomeration, and lack of mechanical support in vivo, researchers have widely combined inorganic selenium or SeNPs with polysaccharide hydrogels, synthetic polymers, or inorganic bioceramic/bioactive glass matrices to construct multiscale carriers and inorganic–organic composite biomaterials.

3.4.1. Polysaccharide-Based Inorganic–Organic Hybrid Hydrogels and Microparticle Systems

Natural polysaccharides are rich in hydroxyl, amino, or carboxyl groups and can stabilize SeNPs through covalent crosslinking, electrostatic interactions, or coordination bonds, endowing the materials with targeting and sustained-release capabilities. For example, Liu et al. first prepared hyaluronic acid (HA)-modified SeNPs via chemical reduction, and then encapsulated them into aldehyde-modified methacrylated hyaluronic acid hydrogel microspheres (HA-SeNPs@AHAMA-HMs) using microfluidic technology and dynamic Schiff base covalent bonds. This system enabled cascade targeted delivery in the articular cavity, but the stability and load-bearing capacity of the hydrogel network under long-term service remained limited [47]. Bai et al. and Zhai et al. used positively charged chitosan (CS) and chitosan oligosaccharide (COS) to stabilize SeNPs during chemical reduction, and combined electrostatic interactions with spray drying to prepare SeNP-loaded composite microparticles (SeNPs-CS-COS-Ms). These microparticles significantly improved selenium retention and in vivo antioxidant bioavailability, though their biological effects fluctuated to some extent in the high-dose range [48,49]. In addition, Ramachandran et al. chemically reduced sodium selenite precursor into zero-valent SeNPs and conjugated them with microbial exopolysaccharides (EPS) using a vortex-ultrasound-assisted dispersion method (SeNPs-EPS). The interfacial C-O-Se coordination/covalent linkages and hydrogen-bonding interactions formed between polysaccharide functional groups and the SeNP surface improved colloidal stability and biocompatibility; however, due to the organic polysaccharide coating, the thermal stability of the conjugate remained relatively limited [50].

3.4.2. Selenium-Doped Bioactive Glasses and Calcium Phosphate-Based Bioceramic Carriers

For orthopedic scenarios requiring hard-tissue conduction and mineralization activity, doping selenium into the lattice of silicate bioactive glasses or calcium phosphate ceramics is a common inorganic composite strategy (although organic templating agents are often used during preparation, the final matrices after high-temperature calcination or precipitation are predominantly inorganic networks). Hu et al. synthesized selenium-doped mesoporous bioactive glass nanospheres (Se-MBG) via a sol–gel process combined with high-temperature calcination, uniformly integrating selenium into the Si–O–Si covalent network. The well-ordered mesoporous structure allowed controlled sustained release of selenium ions and loaded drugs, but the purely inorganic particulate morphology limited its standalone application as a bulk load-bearing scaffold [51]. Similarly, based on the parent ternary silicate-phosphocalcium bioactive glass system (80SiO_2-15CaO-5P_2O_5 mol%), cetyltrimethylammonium bromide (CTAB) was used as an organic supramolecular template to assist the sol–gel process (the organic template was completely removed after calcination), and selenium precursors (SeO_2 or Na_2SeO_3) were substituted for SiO_2 in the nominal synthesis batch (typically 5 mol% substitution, yielding a nominal batch composition of 75SiO_2-15CaO-5P_2O_5-5SeO_2 mol%, where mol% is defined relative to the total moles of network-forming and network-modifying oxides in the synthesis batch). Following high-temperature calcination, during which partial selenium volatilization may occur, making the retained selenium content in the final glass lower than the nominal batch value, selenium is integrated into the final Si-O-Si glass network predominantly as oxidized Se^{4+}/SeO_2-derived network units. The resulting selenium-doped bioactive glass exhibited good mechanical support and apatite mineralization ability; however, the degradation rate of the rigid inorganic glass matrix still tended to mismatch the regeneration rate of loaded drugs or surrounding tissue [52,53]. In a low-temperature calcium phosphate system, Laskus et al. prepared selenium-enriched brushite ($CaHPO_4 \cdot 2H_2O$) via aqueous wet co-precipitation. Selenite ions entered the crystal structure through lattice substitution and P–O–Se bonding, achieving tunable release of selenium ions. However, at higher doping ratios, the loading stability was insufficient [54].

3.4.3. Inorganic–Organic Composite Bone Cement Systems

To combine the operational convenience of clinical bone defect filling with local bioactivity, researchers have introduced selenium-containing components into organic or inorganic–organic hybrid bone cements. Karahaliloğlu and Kilicay stabilized the surface of SeNPs with natural phosphatidylcholine (PC) and then incorporated them into a poly(methyl methacrylate) (PMMA) acrylic bone cement matrix via physical entrapment (PC-SeNPs-PMMA). This composite bone cement exhibited dual functions of good osteoblast compatibility and inhibition of bacterial biofilms, but still faced limitations in antibacterial selectivity and the non-biodegradability of the PMMA organic polymer matrix [55]. Our group previously introduced sodium selenite (Na_2SeO_3) and natural silk fibroin (SF) into degradable calcium phosphate bone cement through a solid–liquid mixed hydration reaction and non-covalent bonding (Se@SF/CPC). The organic silk fibroin phase improved the injectability and anti-washout performance of the bone cement and helped regulate the local release of selenium. Nevertheless, a certain degree of mismatch remained between the long-term degradation cycle of the inorganic cement matrix and the early release rate of selenium ions [13].

In summary, a variety of selenium-containing biomaterial platforms have been developed to date, covering inorganic precursors, elemental selenium nanoparticles, organic selenium dynamic covalent systems, selenium-doped bioactive glasses/ceramics, and in-

organic–organic hybrid composite materials. Different systems have their own advantages and disadvantages in terms of bonding mechanisms, processing characteristics, and biological performance. Table 2 summarizes the classification, synthesis methods, selenium–carrier binding modes, and main advantages and limitations of the representative selenium-containing biomaterials described above.

Table 2. Classification (defined by final matrix composition), synthesis methods, selenium-carrier binding modes, and property comparisons of representative selenium-based biomaterials.

Material Category	Material System	Se Species & Binding	Synthesis Method	Advantages	Limitations	Ref.
Inorganic Se precursors and elemental nano-Se	Na_2SeO_3	Selenite ion; water-soluble salt or physical blending	Commercial inorganic salt precursor	Good solubility, readily available, rapid selenium release	Narrow therapeutic window, high-dose burst cytotoxicity	[29–31]
	SeNPs	Zero-valent selenium nanoaggregates with surface stabilizers	Chemical reduction, laser ablation, biological reduction	Higher bioavailability, lower acute toxicity than free selenite	Prone to aggregation and deactivation, ultrasmall particles still cytotoxic	[35,36]
Organic Se compounds and dynamic covalent materials	Selenoether-based HOF nanozymes	Organic selenoether moieties (stable covalent Se–C bonds) integrated into hydrogen-bonded organic frameworks	Supramolecular self-assembly and peptide surface functionalization	High bond stability, intrinsic multienzyme cascade antioxidant activity, good biocompatibility	Relatively complex multi-step organic/framework synthesis; not yet evaluated in load-bearing orthopedic defects	[43]
	Diselenide-bridged materials (DSeD, Se-Se-MSNs)	Diselenide covalent bonds integrated into prodrugs or mesoporous silica	Condensation reaction or silane crosslinking	Redox-responsive drug release, self-healing potential	Premature degradation under strongly oxidative conditions	[44,45]
	Selenourea derivatives	Selenourea functional groups covalently bonded	Room-temperature organic synthesis	In vitro radical scavenging and antibacterial activity	Limited to small-molecule in vitro evaluation, no bulk scaffold data	[46]
Pure inorganic Se-doped bioceramics and bioglasses	Se-MBG	Selenium oxide doped into silicate glass network	Sol–gel combined with high-temperature calcination	Large mesoporous surface area, controlled ion and drug release	Brittle inorganic particles, limited load-bearing capacity alone	[51]
	Se-doped bioactive glass (parent glass: $80SiO_2$-$15CaO$-$5P_2O_5$ mol%; nominal Se-substituted batch: $75SiO_2$-$15CaO$-$5P_2O_5$-$5SeO_2$ mol%)	Precursor: 5 mol% SeO_2 or Na_2SeO_3 substituted for SiO_2 in the nominal synthesis batch (mol% relative to total batch oxide moles). Final material: oxidized Se^{4+}/SeO_2 units integrated into the calcined Si-O-Si glass network (partial volatilization during calcination; CTAB template completely removed)	CTAB-templated sol–gel and high-temperature calcination	Good biomineralization activity and pore structure stability	Degradation rate mismatch with soft tissue or organic drugs	[52,53]

	Se-enriched brushite	Selenite ion partial lattice substitution of phosphate via P–O–Se linkage (purely inorganic matrix without organic components)	Aqueous wet co-precipitation	Good osteoconductivity and tunable selenium release	Substitution limited by lattice stability; high doping alters crystallinity	[54]
Inorganic-organic hybrid composite biomaterials	HA-SeNPs@AHAMA-HMs	Zero-valent SeNPs (reduction product from Na_2SeO_3 precursor) stabilized by HA and encapsulated in AHAMA hydrogel microspheres via Schiff base bonds	Chemical reduction of Na_2SeO_3 followed by microfluidic crosslinking	CD44 cascade targeting of chondrocytes, stable sustained release	Low mechanical strength, not suitable for load-bearing bone defects	[47]
	SeNPs-CS-COS-Ms	Zero-valent SeNPs (reduction product from Na_2SeO_3 precursor) embedded in chitosan/chitooligosaccharide matrix via electrostatic interactions	Chemical reduction of Na_2SeO_3 and spray drying	Good selenium retention and gastrointestinal biocompatibility	Release effects fluctuate at high doses	[48,49]
	SeNPs-EPS	Zero-valent SeNPs (reduction product from Na_2SeO_3 precursor) conjugated to microbial exopolysaccharide via C-O-Se coordination/covalent and hydrogen bonding	Chemical reduction of Na_2SeO_3 and vortex-ultrasound-assisted conjugation	Good biocompatibility, high colloidal stability	Weak thermal stability of polysaccharide coating	[50]
	PC-SeNPs-PMMA	Phosphatidylcholine-stabilized zero-valent SeNPs (reduction product) physically entrapped in PMMA bone cement matrix	Chemical reduction with phosphatidylcholine stabilization and PMMA polymerization	Combined mechanical fixation with local antibacterial and osteogenic activity	Non-biodegradable, nanoparticle release concentrated at surface	[55]
	Se@SF/CPC	Unreduced selenite ions (SeO_3^{2-} from Na_2SeO_3 precursor) and silk fibroin co-dispersed in calcium phosphate cement via non-covalent hydration interactions	Solid–liquid mixing and self-setting hydration reaction	Good injectability, local sustained release, and osteoconductivity	Temporal mismatch between cement degradation and early selenium release	[13]

Note: Material categories are defined according to the final chemical composition of the prepared matrices. In the pure inorganic bioceramic/bioglass category, organic templates used during sol–gel processing (e.g., CTAB) are completely removed via high-temperature calcination, and Se-enriched brushite is synthesized in a purely aqueous system without organic additives.

4. The Effect of Se-Containing Biomaterials in Regulating Osteoblasts and Osteoclasts

Se levels and selenoproteins play a key role in keeping bone homeostasis stable and stopping pathological bone loss [56]. When stimulated by 1α,25-dihydroxyvitamin D3, TXNRD1 controls osteogenic factors like RUNX2 and Sp7. This improves ALP activity, osteocalcin production, and matrix mineralization [57,58]. GPX1 is a main antioxidant en-

zyme in osteoclasts. Estrogen signaling raises its expression, and it inhibits osteoclast formation through the RANKL/RANK pathway [58]. This coordinated system keeps bone remodeling balanced and supports skeletal tissue repair.

The Se–GPX4–ferroptosis defense axis is another key pathway that Se-containing biomaterials use to protect the skeleton. Se is a necessary cofactor for GPX4, the core regulator of ferroptosis. Ferroptosis is a type of iron-dependent programmed cell death caused by lipid peroxidation. It is linked to osteoporosis, osteoarthritis, and intervertebral disc degeneration. Se released from biomaterials boosts GPX4 activity. This turns on the Se–GPX4–ferroptosis axis, which clears lipid peroxides, stops ferroptosis in chondrocytes, osteoblasts, and nucleus pulposus cells, and protects skeletal lineage cells [59].

4.1. Regulation of Osteoblast Differentiation and Bone Formation

High-level oxidative stress represents a primary antagonist of bone regeneration by impairing progenitor cell commitment. To counteract these deleterious effects, Sharma et al. exposed MC3T3-E1 pre-osteoblasts to Na_2SeO_3 in an H_2O_2-induced oxidative stress environment. Na_2SeO_3 boosted osteogenic progression, ALP activity, and the expression of key transcription factors and differentiation markers. Further tests showed that Na_2SeO_3 activates Wnt/β-catenin signaling by inhibiting GSK-3β, stabilizing β-catenin, and increasing Axin-2 reporter activity, whereas pharmacological blockade with the Wnt antagonist DKK1 abrogated these pro-osteogenic effects, confirming functional dependence on the Wnt/β-catenin pathway [60]. In line with these results, Sahin et al. investigated selenomethionine (SeMet), a natural organoselenium compound found in biological systems. It improves the survival of human fetal osteoblasts and increases calcium deposition in a dose-dependent way [61].

Redox balance is essential for the targeted differentiation of human mesenchymal stem cells (hMSCs). Investigating this delicate balance, Fatima et al. found that SeNPs guide hMSCs to differentiate into osteoblasts instead of adipocytes. They increase osteogenic transcription factor levels, speed up matrix mineralization, and reduce lipid droplet formation and adipogenic markers. These effects are linked to SeNPs' ability to inhibit ROS accumulation and enhance endogenous antioxidant defenses during osteogenic induction. SeNPs treatment also concurrently elevated the phosphorylation levels of JNK and FOXO3a. Although direct causal dependence remains to be verified by genetic knockdown or specific pharmacological inhibitor experiments, this correlation suggests the JNK/FOXO3a axis as a candidate pathway associated with SeNP-induced osteogenic differentiation [62].

Diabetic bone disease is a serious complication caused by metabolic disorder and redox imbalance. In this disease, ROS breaks the coupling between angiogenesis and osteogenesis. Addressing this complex pathophysiology, Wu et al. prepared Se-doped carbon quantum dots (SeYCQDs) from Se-rich yeast using a hydrothermal method. This method makes use of the natural conversion of inorganic Se into bioavailable organoselenium metabolites. SeYCQDs function as a dual-function nanozyme with GPX-mimicking activity. Under high glucose conditions, they catalytically clear ROS to restore mitochondrial membrane potential in vascular endothelial cells, reversing endothelial dysfunction. Concurrently, SeYCQDs treatment was accompanied by upregulated expression of components within the VEGFA/BMP2/Noggin signaling axis, which correlated with enhanced type H vessel formation and osteoblast differentiation to rebuild angiogenic–osteogenic coupling [63].

4.2. Regulation of Osteoclast Differentiation and Bone Resorption

Osteoclast hyperactivation drives bone loss in disorders with elevated oxidative stress. Se-containing biomaterials can suppress osteoclast differentiation by activating antioxidant selenoproteins that scavenge ROS [64].

Osteoclasts also mediate tumor-induced osteolysis, in which tumor-derived factors overactivate osteoclast differentiation and resorption, causing major bone destruction. Establishing the clinical relevance of Se in this pathology, Zhang et al. evaluated various Se donors, including organic Se and SeNPs, in tumor-induced osteolysis. Clinical observational data indicated lower dietary Se intake in breast cancer patients with bone metastasis than in those without. In preclinical cell and animal models, SeNPs exerted dual effects: they induced cytotoxicity in breast cancer cells and suppressed osteoclast progenitor survival and differentiation in association with IL-6 downregulation, interrupting the vicious cycle of osteolysis [65]. Building upon this targeted niche intervention, Zou et al. designed zeolitic imidazolate framework-8-capped copper selenide nanocomposites (ICG@$Cu_{2-X}Se$-ZIF-8) to target the bone metastatic niche. In this multi-component platform, indocyanine green (ICG) and $Cu_{2-x}Se$ mediated photothermal tumor ablation, while metabolically released Se contributed to regulating redox homeostasis and upregulating selenoproteins in osteoclasts. Together, the nanocomposites reduced osteoblast RANKL expression, inhibited RANKL-induced signaling in bone marrow monocytes, and suppressed IL-8 secretion to attenuate tumor-driven osteolytic bone loss [66].

At the molecular level, the regulatory influence of Sec incorporation on osteoclast function is intricately linked to the activity of selenoprotein W (SELENOW). Defining this mechanism, Kim et al. reported that Sec-mediated regulation of osteoclasts involves SELENOW. Selenow-deficient mice show a high bone mass phenotype from impaired resorption, whereas transgenic overexpression causes osteoporosis due to excessive bone loss. SELENOW overexpression enhances osteoclastogenesis in vitro by promoting nuclear translocation of NF-κB and NFATc1, whereas genetic ablation of Selenow suppresses osteoclast formation [67].

5. The Effect of Se-Containing Biomaterials in Regulating Chondrocyte Differentiation

KBD is a nutritionally linked endemic osteoarthropathy characterized by progressive chondrocyte apoptosis and uncontrolled ECM degradation. Se deficiency is widely recognized as a primary environmental cause [68]. To address this deficit at the cellular level, Wang et al. showed that Se supplementation restores matrix homeostasis by shifting metabolism from catabolism to anabolism: it increases type II collagen, aggrecan, and sulfated glycosaminoglycans while suppressing matrix metalloproteinases. Se also reduces cytotoxic injury in stressed chondrocytes by inhibiting aberrant Wnt/β-catenin activation, defining a Se-dependent protective circuit that preserves cartilage under degenerative conditions [69].

Cartilage has limited regenerative capacity after injury or degeneration, making durable repair a persistent clinical challenge. Addressing the limitations of conventional scaffolds, Han et al. constructed chondroitin sulfate A–functionalized SeNPs (CSA-SeNPs) by supramolecular self-assembly between Na_2SeO_3 and negatively charged CSA, stabilized by electrostatic interactions and hydrogen bonding. In chondrocyte co-culture, these high-Se-loading nanostructures promote proliferation and cartilage-specific matrix synthesis. The design combines CSA bioactivity with SeNP redox modulation in one platform, with better biocompatibility than free Na_2SeO_3. Low-dose CSA-SeNPs also outperform inorganic selenium in rat cartilage lesion repair [70]. Quantitative proteomics enrichment analysis showed that CSA-SeNP-treated chondrocytes exhibited coordinated

changes in proteins and candidate pathways related to ribosome biogenesis, mRNA surveillance, ER-associated protein processing, endocytic trafficking, and autophagy, suggesting that CSA-SeNPs may enhance the stress resistance of diseased chondrocytes by alleviating ER stress and improving biosynthetic homeostasis [71].

Selenoproteins regulate multiple homeostatic programs in chondrocytes, including redox defense, inflammatory resolution, and ferroptosis. Illustrating these protective effects, Hu et al. showed that phycocyanin-functionalized SeNPs protect chondrocytes in osteoarthritis through combined antioxidant buffering and ferroptosis suppression. In IL-1β-stimulated ATDC5 cells, comparing phycocyanin-SeNPs with unfunctionalized precursors demonstrated that these nanoparticles effectively scavenge ROS, reduce labile Fe^{2+} accumulation and lipid peroxidation, upregulate ferroptosis-resistance markers (GPX4 and SLC7A11), and modulate MAPK pathway phosphorylation [72]. The same group reported that SeMet supports GPX4-dependent anti-ferroptosis defense in chondrocytes. GPX4 is an antioxidant enzyme with selenocysteine (Sec) at its active center. Selenomethionine (SeMet) released from the hydrogel serves as an organic selenium source, providing active selenium precursors via transsulfuration and selenium metabolism pathways in chondrocytes, thereby supporting GPX4 biosynthesis and enhancing its anti-ferroptosis function [73].

Selenoproteins protect chondrocytes from oxidative stress and maintain ECM metabolic homeostasis. GPX1 is particularly important for cartilage development, osteoarthritis progression, and articular cartilage degeneration. Knocking down Gpx1 in ATDC5 cells reduces glycosaminoglycan accumulation and cell proliferation, and downregulates chondrogenic markers such as SOX9, collagen type II, and aggrecan. GPX1 depletion also causes both oxidative and reductive stress, with excess ROS and an abnormally high GSH/GSSG ratio. The chondrogenesis impairment from GPX1 silencing resembles Se-deficient endemic osteoarthropathy and can be rescued by the chemical chaperone diamide, confirming that redox imbalance rather than general cytotoxicity drives the differentiation failure [74]. In the upstream regulation of these selenoenzymes, it is important to distinguish between the two selenophosphate synthetase paralogs: canonical selenophosphate synthetase 2 (SEPHS2) is itself a Sec-containing selenoprotein that directly catalyzes selenophosphate synthesis from selenide and ATP, whereas selenophosphate synthetase 1 (SEPHS1) neither contains Sec nor directly catalyzes selenophosphate synthesis, functioning instead as an essential non-selenoprotein regulator of cellular redox homeostasis [75]. Specifically, Kang et al. demonstrated that SEPHS1 expression is significantly downregulated in human and murine osteoarthritic cartilage; chondrocyte-specific *Sephs1* deficiency in mice selectively impaired the expression of oxidoreductase selenoproteins (such as GPX1 and SELENOW), resulting in excessive ROS accumulation, cellular senescence, and accelerated OA cartilage destruction [76].

6. Immunomodulatory Functions of Se-Containing Biomaterials

Acute inflammation starts the repair process: it clears dead tissue debris and recruits repair progenitor cells through anabolic signals. Chronic inflammation works the opposite way. It creates a catabolic, high oxidative stress microenvironment that breaks down tissue matrix and stops regeneration [77]. Highlighting the systemic relevance of these processes, Al-Mubarak et al. compared serum Se levels with multiomic profiles of peripheral blood mononuclear cells from heart failure patients. Integrated bioinformatics analysis found that processes controlling leukocyte differentiation, activation, and cytokine production were enriched. This observational multiomic analysis suggests that circulating Se status is closely associated with systemic immunoregulatory pathways in clinical cohorts, although causal immunomodulatory efficacy requires direct experimental verification [78].

In long-term inflammatory sites, built-up reactive oxygen and nitrogen species (RONS) damage mitochondria and slow down cellular respiration. This pushes M1 macrophages to rely on aerobic glycolysis (the Warburg effect) even when oxygen is sufficient [79]. This glycolysis-dominant metabolic state helps sustain the pro-inflammatory signaling cascade associated with M1 macrophages. In contrast, the polarization and functional maintenance of anti-inflammatory, pro-repair (M2-like) macrophages are typically accompanied by enhanced mitochondrial oxidative phosphorylation (OXPHOS) and tricarboxylic acid (TCA) cycle flux [80]. It should be noted that the necessity of metabolic pathways for macrophage polarization depends on the specific stimulating factors and functional endpoints. For example, Divakaruni et al. demonstrated that direct inhibition of OXPHOS does not block IL-4-induced expression of specific M2 surface markers and genes in bone marrow-derived macrophages (BMDMs) in vitro [81]. However, in the microenvironment of chronic inflammation and tissue injury, restoring mitochondrial respiratory homeostasis and redox balance still plays an important supporting role in maintaining macrophage metabolic flexibility, preventing sustained RONS bursts, and promoting functional resolution of inflammation in vivo [80].

Macrophages are central to both starting and ending inflammation. Se-modified materials adjust the redox balance inside macrophages. They cut down the sharp RONS increase when inflammation first starts, helping inflammation fade on time and supporting tissue repair. Se-doped mesoporous bioactive glass (Se-MBG) scaffolds steer macrophages toward oxidative phosphorylation. They also raise GPX4 levels to keep mitochondrial energy metabolism steady and hold back oxidative bursts. This immunometabolic reprogramming builds a microenvironment that supports regeneration, combining immune regulation with better bone repair [82].

Mitochondrial hypoxia and RONS buildup in macrophages also throw off local redox balance. Chen et al. made a Janus-structured nanomachine (Pd@MSe) by embedding palladium single-atom nanozymes into porous Se carriers. In the rheumatoid arthritis microenvironment, the oxygen evolution reaction pushes the nanomachine into macrophage mitochondria. The single-atom catalytic sites speed up electron transfer. This strengthens GPX-mimicking activity and self-propulsion, and quickly brings local oxygen levels back to normal. This Se-based platform stopped the inflammatory chain reaction, kept mitochondrial respiration stable, and reduced cartilage damage. It offers a disease-modifying treatment strategy for rheumatoid arthritis [83].

Se-containing biomaterials exert immune-regulating effects by fully reprogramming macrophage metabolism. They boost metabolic flow through the pentose phosphate pathway, tricarboxylic acid cycle, and oxidative phosphorylation. This function depends on a working selenoproteome. When selenoproteins are deficient, cells lose their metabolic flexibility. When succinate dehydrogenase is inhibited by dimethylmalonate, the Se-dependent regulatory circuit is disrupted, and inflammation resolution is delayed in a mouse peritonitis model. This finding confirms that normal mitochondrial respiration is necessary for inflammation to resolve properly. Therefore, Se availability guides macrophages to develop anti-inflammatory and repair-promoting features by adjusting key metabolic checkpoints [84].

At the molecular level, SELENOW controls the expression of other selenoproteins, maintains redox balance, and stabilizes mitochondrial energy metabolism to regulate inflammation. In macrophages derived from Selenow-knockout mouse bone marrow, ARG1 expression drops. This weakens M2 polarization and slows down timely inflammation resolution. Neutrophil efferocytosis also declines, which dampens pro-resolving signals. Selenow deficiency also breaks the normal glycolytic switch that happens when macrophages activate. It makes cells abnormally rely on oxidative phosphorylation to produce ATP, even when there is plenty of glucose [85].

Pushing the boundaries of systemic Se delivery, Ouyang et al. designed an oral delivery platform of hyaluronic acid-modified SeNPs encapsulated in calcium alginate hydrogel microbeads to enable in situ biosynthesis of functional selenoproteins in the gastrointestinal tract. In colitis models, this system suppressed pro-inflammatory cytokine secretion and reshaped the immune cell landscape, reducing neutrophils and monocytes while expanding regulatory T cells. This in situ synthesis strategy avoids the proteolytic instability and storage challenges of conventional oral protein delivery, offering a physiologically compatible approach for inflammation-driven diseases [86]. Osteomyelitis is constrained by persistent bacterial colonization, hyperactive inflammation, and impaired osteogenesis. Cai et al. built a multifunctional nanoplatform (Se-CD@Cu-EGC) by integrating Se-doped carbon dots into a copper-epigallocatechin gallate (Cu-EGC) metal-phenolic network. Comparative evaluation of the platform components indicated that the Cu-EGC network contributed broad-spectrum antibacterial activity, while the Se-doped carbon dots scavenged excess ROS and promoted macrophage repolarization from the M1 to M2 phenotype; concurrently, the optimized surface charge was associated with activation of the BMP/Smad signaling axis to enhance osteogenic differentiation, jointly resolving the infection-associated inflammatory microenvironment [87]. The relevant signaling pathways and specific mechanisms are summarized in Table 3.

Table 3. Cellular effects mediated by selenium-containing biomaterials.

Cell Types	Biomaterials	Delivered/ Released Se Species	Mechanism Category & Evidence Strength	Related Pathways/Key Molecules	Biological Effects	References
Osteoblasts	Na_2SeO_3	Selenite ion (SeO_3^{2-})	Exogenous inorganic Se treatment; pathway activation with inhibitor validation	Wnt/β-catenin pathway; RUNX2, Sp7, ALP	Promotes osteogenic differentiation and matrix mineralization under H_2O_2 stress	[60]
	SeMet	Selenomethionine (organic Se)	Exogenous organic Se supplementation; phenotype and survival association	Cell survival and calcium deposition-related pathways	Dose-dependently increases human fetal osteoblast survival and calcium nodule deposition	[61]
	SeNPs	Zero-valent SeNPs (intracellular thiol reduction to selenide)	Nano-Se antioxidant intervention; protein phosphorylation correlation evidence (candidate pathway)	ROS scavenging; elevated JNK/FOXO3a phosphorylation	Promotes hMSC osteogenic differentiation and inhibits adipogenic differentiation	[62]
	SeYCQDs	Se-enriched yeast-derived carbon quantum dots (Se-containing organic functional groups)	Intrinsic GPX-mimicking nanozyme catalytic activity + candidate pro-angiogenic/osteogenic signaling axis	Intrinsic GPX-mimicking activity; VEGFA/BMP2/Noggin axis	Catalytically scavenges high glucose-induced ROS, restores endothelial mitochondrial potential, and rebuilds angiogenesis-osteogenesis coupling	[63]

Osteoclasts	LNT-Se	Surface-active zero-valent SeNPs (metabolically converted to Sec)	Endogenous selenoprotein upregulation + downstream signal inhibition	GPX1 upregulation; inhibition of NF-κB/NFATc1 pathway	Promotes macrophage repolarization, inhibits osteoclastogenesis and pathological osteolysis	[64]
	SeNPs	Zero-valent SeNPs/organic Se donors	Cytokine downregulation and phenotype inhibition	Downregulation of IL-6 expression	Induces tumor cytotoxicity and inhibits osteoclast progenitor differentiation, interrupting the vicious cycle of osteolysis	[65]
Chondrocytes	CSA-SeNPs	Chondroitin sulfate A-functionalized zero-valent SeNPs	Composite nanoparticle intervention ([70]) + quantitative proteomics enrichment correlation analysis (candidate pathway, [71])	Ribosome biogenesis, mRNA surveillance, ER stress, and autophagy-related protein networks	Promotes chondrocyte proliferation and matrix synthesis, improves rat cartilage defect repair	[70,71]
	Phycocyanin-SeNPs	Phycocyanin-functionalized zero-valent SeNPs	Antioxidant buffering + ferroptosis marker expression regulation	Scavenges ROS and labile Fe^{2+}; upregulates GPX4, SLC7A11, and modulates MAPK pathway	Inhibits lipid peroxidation and chondrocyte ferroptosis, delays rat OA progression	[72]
	SeMet-releasing composite hydrogel (with Fe^{2+}-capturing nanocatalysts)	Selenomethionine (SeMet, organic Se amino acid)	Metabolic Se precursor supply supporting Sec-containing GPX4 biosynthesis + accompanying Fe^{2+} chelation + associated signaling pathway changes	Transsulfuration/Se metabolism supporting GPX4 synthesis; PI3K/Akt/FOXO1 axis	Inhibits chondrocyte lipid peroxidation and ferroptosis, restores mitochondrial homeostasis, and attenuates OA cartilage degeneration	[73]
	WYRGRL-targeted KGN@DSeD self-assembled nanoparticles	Cleaved diselenide-bridged diclofenac prodrug (DSeD) metabolites	Redox-responsive diselenide bond cleavage for targeted cargo release + associated NRF2 pathway activation + complementary drug/KGN effects	ROS-triggered Se-Se bond cleavage; NRF2 antioxidant signaling; kartogenin-induced chondrogenesis	Provides sustained intra-articular retention, anti-inflammatory analgesia, antioxidant defense, and cartilage matrix repair in OA mice	[45]
Immune cells	Se-MBG	Se ions released from Se-doped mesoporous bioactive glass	Se ion release + immunometabolic reprogramming and endogenous GPX4 upregulation	Promotes oxidative phosphorylation (OXPHOS); upregulates GPX4	Inhibits oxidative burst, promotes macrophage M2 polarization, and enhances bone regeneration	[82]

Pd@MSe	Porous Se carrier loaded with palladium single-atom nanomachines	Single-atom synergistic GPX-mimicking nanozyme catalysis and oxygen evolution activity	Intrinsic GPX-mimicking catalytic activity, mitochondrial targeting, and oxygen evolution reaction	Alleviates mitochondrial hypoxia and RONS accumulation, blocks inflammatory cascade, and reduces cartilage destruction	[83]

7. Se-Containing Biomaterials for Musculoskeletal System Disorders

7.1. Application of Se-Containing Biomaterials in the Treatment of Osteoporosis

Osteoporosis is a systemic skeletal disorder divided into primary forms (mainly postmenopausal and senile) and secondary forms with distinct causes. Its main clinical consequence is increased bone fragility from reduced BMD and compromised microarchitecture, making fractures likely even after minimal trauma [88]. Clinical observational studies have shown that serum selenium levels are positively correlated with BMD and negatively correlated with the prevalence of osteoporosis. Epidemiological meta-analyses also indicate that higher dietary selenium intake is associated with a lower risk of hip fracture. However, these observational associations still require further validation by randomized controlled clinical intervention trials [89]. Conversely, in third-generation telomerase knockout (G3 Terc$^{-/-}$) mice with a short-telomere background, long-term dietary selenium deprivation accelerates age-related glucose intolerance, reduced insulin sensitivity, and insufficient insulin secretion, and induces premature aging-related phenotypes such as osteoporosis (deterioration of trabecular bone microarchitecture), premature hair graying, hair loss, and cataracts (note that these phenotypes were observed in the specific genetic context of telomere dysfunction) [90].

Translating these biological insights into engineered therapeutics, Zou et al. engineered lentinan-modified surface-active SeNPs (LNT-Se) that facilitate cellular uptake and metabolic conversion to Sec. In vivo, LNT-Se outperformed native Sec by upregulating GPX1, which suppresses osteoclastogenesis and pathological osteolysis (Figure 3A,B) [64]. Bone microarchitecture deterioration in osteoporosis is also linked to ferroptosis-induced impairment of osteoblast matrix secretion. To intercept this destructive cascade, Cao et al. designed bone-targeted alendronate-modified Se-doped carbon dots (ASCDs). In OVX mice, ASCDs reversed trabecular bone loss by reducing osteoblast ferroptosis and enhancing osteogenic differentiation. They activate the intracellular GSH/GPX4 antioxidant axis, suppressing lipid peroxidation and restoring mitochondrial function to promote mineralized nodule formation (Figure 3C,D) [91]. Thus, Se-dependent selenoprotein activation is a key node regulating the coupled differentiation of osteoblasts and osteoclasts, providing a molecular basis for treating estrogen deficiency-induced osteoporosis.

Osteoporotic fracture healing is often complicated by prolonged recovery, inadequate regeneration, and high nonunion rates. These challenges arise from a systemic catabolic state with excessive osteoclast resorption and insufficient osteoblast formation, which compromise structural integrity and disrupt signaling needed for regeneration [92]. We previously developed a Se-modified bone cement (Se@SF/CPC) by integrating sodium selenite and silk fibroin into calcium phosphate cement to counteract oxidative stress in the osteoporotic microenvironment. Implanted into critical-sized distal femoral defects in OVX rats, the cement enhanced new bone formation and bone volume fraction, associated with local GPX1 upregulation. The osteoconductive composite provides sustained local Se release, avoiding the limitations of systemic administration and rescuing the impaired

osteogenic potential of endogenous stem cells (Figure 3E,F) [13]. Utilizing a similar localized strategy, Huang et al. developed an injectable poly(lactide-carbonate)/β-TCP composite loaded with SeNPs (PDT-TCP-SE). Injected into femoral condyle defects in OVX rats, it promoted mineralized deposition and reconstructed trabecular architecture, accelerating bone healing (Figure 3G,H) [93].

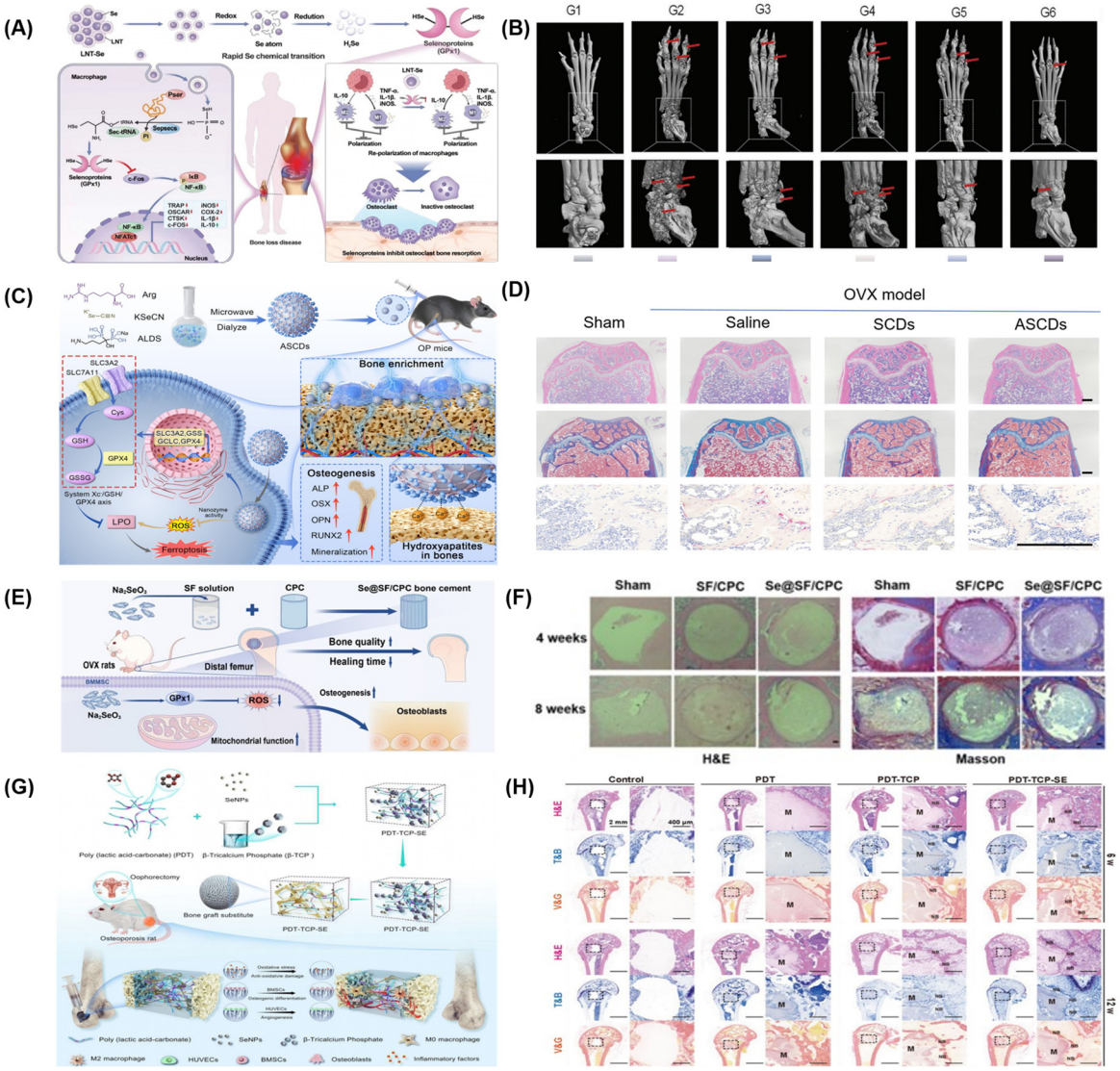

Figure 3. Applications of selenium-containing biomaterials in osteoporosis. (**A**,**B**) SeNPs promote macrophage repolarization to suppress osteoclasts and protect against bone loss. (**A**) Schematic of rapid activation of selenoproteins by Se nanoparticles and modulation of macrophage repolarization to inactivate osteoclasts. (**B**) Representative hind-paw 3D micro-CT images. (**A**,**B**) Reprinted with permission from Ref. [64]. License Number: 6311661015870. Copyright 2024, Elsevier. Red arrows indicate bone destruction. (**C**,**D**) ASCDs suppress ferroptosis to rescue bone loss in osteoporosis. (**C**) Schematic illustration of the synthesis of ASCDs and molecular mechanisms for OP treatment through inhibition of ferroptosis. (**D**,**H**,**E**) Staining of the distal part of the femur. Masson staining of the distal part of the femur. Representative images of TRAP staining in the distal part of the femur (scale = 200 μm). (**C**,**D**) Reprinted with permission from Ref. [91]. License Number: 6311661420806. Copyright 2026, Elsevier. (**E**,**F**) Se@SF/CPC cement activates GPx1 to accelerate bone repair in osteoporosis. (**E**) Selenium-functionalized SF/CPC cement enhances bone healing in ovariectomized rats by activating GPx1 to suppress oxidative stress and promote osteogenesis. (**F**) Representative histological images of rat femurs using hematoxylin and eosin (**H**,**E**), and Masson staining. (**E**,**F**) Adapted from Ref. [13] under the terms of the Creative Commons Attribution License (CC

https://doi.org/10.3390/antiox15121545

BY). (**G**,**H**) Radiographic and histologic evaluation of osteoporotic bone healing enhanced by the PDT-TCP-SE bioactive scaffold. (**G**) The detailed method and process of fabricating PDT-TCP-SE bone graft substitute material and the mechanism of bone regeneration at osteoporotic bone defect by the injectable bone graft substitute material. (**H**) H-E, T-B and V-G staining of undecalcified femoral condyle sections at 6 and 12 weeks after implantation. (**G**,**H**) Adapted from Ref. [93] under the terms of the Creative Commons Attribution License (CC BY).

7.2. Se-Containing Biomaterials for Bone Regeneration

Bone injury is a common orthopedic challenge including traumatic fractures, inflammation-mediated bone loss, post-tumor resection defects, and implant-related osseointegration failure. Autologous grafts, the current mainstay, have donor site morbidity and limited availability, while allogeneic grafts carry risks of immune rejection and disease transmission [94]. Single-modality therapies also often fail to address the multifactorial nature of complex injuries involving inflammation, infection, tumor recurrence, and deficient regeneration [95]. Se-containing biomaterials offer a versatile solution because their morphology and dosage can be tailored to different clinical scenarios, from local periodontal injection to implant coating and bulk defect filling. They also integrate well with polymer, ceramic, and metallic systems without compromising mechanical integrity or degradation.

Inflammatory bone defects are hard to treat because long-lasting inflammation goes along with poor tissue regeneration. Addressing this hostile niche, He et al. developed Se-doped bioactive glass nanoparticles. These particles reprogram macrophage metabolism and build a microenvironment that supports tissue repair. In mouse models of inflammatory skull defects, the nanoparticles lowered TNF-α levels and raised ARG1 levels. They also boosted osteogenic differentiation and increased bone matrix deposition. The particles produce anti-inflammatory effects by interacting with cytokine receptors, which neutralize pro-inflammatory substances. Steady Se ion release was also associated with macrophage metabolic reprogramming through modulation of the NRF2/NF-κB signaling axis, restoring mitochondrial function and promoting transition toward the pro-healing M2 phenotype [96].

Excess ROS inhibits osteogenic differentiation in periodontal tissues, hindering regeneration. Zou et al. engineered a Se-albumin corona rinse (H@SeNPs) through albumin/nano-Se assembly. These nanoparticles enhanced osteogenic differentiation in hyperglycemic microenvironments and improved periodontal bone regeneration primarily through ROS scavenging, which was accompanied by TXNRD1 upregulation and downstream β-catenin signaling activation [97]. In the context of compromised osseointegration following titanium implantation, Jiang et al. developed a multifunctional composite hydrogel coating with immunomodulatory, antioxidant, and osteogenic functions. The coating blends Laponite with SeNPs, then photocrosslinks with CMCSMA and GelMA to form a strong adhesive layer on titanium. In a rat distal femoral defect model, comparative evaluation of the coating components indicated that SeNPs primarily contributed to ROS scavenging and macrophage polarization toward the pro-healing M2 phenotype, whereas the Laponite component provided an incremental pro-osteogenic effect by promoting bone matrix mineralization (Figure 4A,B) [98].

After osteosarcoma surgery, scaffolds need to handle two core tasks at once: eliminate leftover tumor cells and repair large segmental bone defects. Tackling this dual imperative, Bian et al. developed a layered double hydroxide Se nanocomposite (LDH/Se) loaded onto a bioactive glass scaffold (BGS@LDH/Se) for post-operative treatment. Negatively charged SeNPs are evenly spread across nanosheet surfaces, which stops them from clumping together and losing activity. Comparisons among bare BGS, selenium-free BGS@LDH, and BGS@LDH/Se demonstrated that while the BGS@LDH matrix provided

structural support, the incorporated SeNPs specifically conferred antitumor cytotoxicity, antibacterial efficacy, and enhanced osteogenesis (Figure 4C–E) [14]. Pursuing an alternative multimodal design, Xu et al. fabricated a germanium-selenium co-doped piezoelectric PLA nanofiber membrane coated onto a TCP bioceramic scaffold (TCP-PLA/GeSe) to mimic the native periosteum. In a rabbit large segmental bone defect model, comparative evaluation with and without ultrasound (US) and near-infrared (NIR) irradiation showed that US-triggered piezoelectric stimulation from the PLA/GeSe membrane promoted neurogenic and osteogenic regeneration, while NIR-induced photothermal conversion and Se release jointly contributed to osteosarcoma ablation in vivo (Figure 4F,G) [99]. One major drawback of TCP ceramic-polymer composites is insufficient mechanical strength. They cannot support load-bearing uses like femur or tibia reconstruction.

Local infection is a common and serious complication of bone defects. It comes from surgical contamination, bacterial invasion, or blood-borne spread, and often causes chronic pain, repeated infection, delayed bone healing, or permanent disability [100]. SeNPs have natural antibacterial effects and bone-promoting potential. This makes them useful for treating infectious bone defects [32]. Using the potent inherent antimicrobial properties and osteoinductive potential of SeNPs, Lei et al. developed ultrasound-responsive Se-modified barium titanate nanoparticles (Se@BTO). These nanoparticles killed Staphylococcus aureus and repaired infected femoral condyle defects in rats, boosting bone regeneration [101]. Addressing the specific challenge of implant-related osteomyelitis, Mao et al. designed a Se-doped nanoparticle coating for zinc-based implants (Se-CPS) for combined treatment. In the Se-CPS coating, comparison among pure zinc (Zn), selenium-free calcium phosphate silicate coating (CPS), and selenium-doped coating (Se-CPS) showed that the early antibacterial effect was mainly attributed to zinc ion release and the local alkaline microenvironment, while the incremental contribution of selenium doping was to restore host cell viability, enhance macrophage xenophagy, and promote M1-to-M2 polarization by upregulating endogenous Sec-containing selenoproteins (such as GPX1, GPX4, and TXNRD1) alongside the non-selenoprotein upstream redox regulator SEPHS1 (Figure 4H,I) [102].

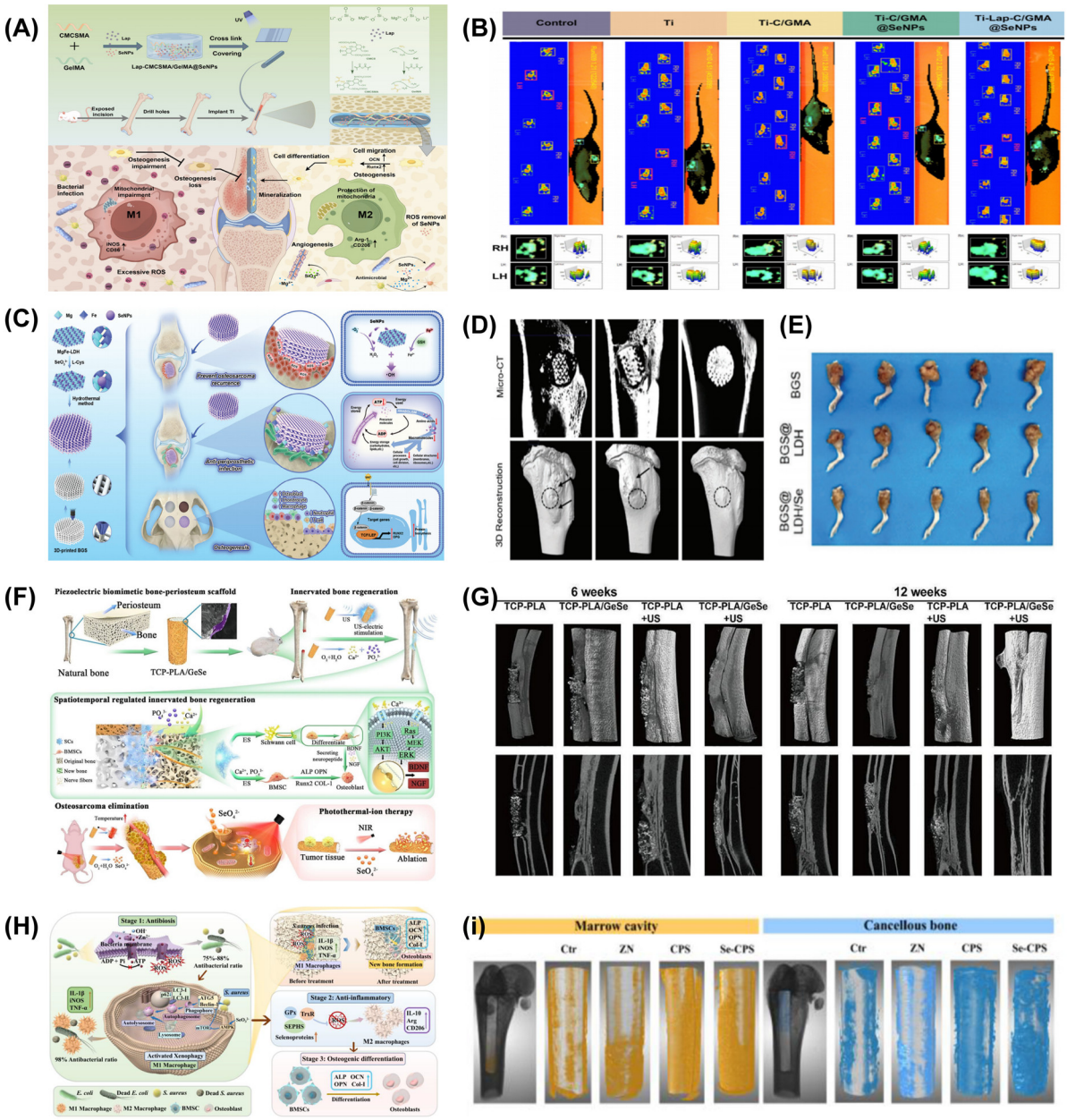

Figure 4. Applications of selenium-containing biomaterials in injury treatment. (**A**,**B**) Development of a multifunctional Lap-CMCSMA/GelMA@SeNPs hydrogel coating for enhancing bone regeneration and functional recovery in femoral defect repair. (**A**) This figure illustrates the fabrication process of the Lap-CMCSMA/GelMA@SeNPs composite hydrogel coating, which demonstrates antibacterial activity, ROS scavenging capability, anti-inflammatory properties, angiogenic potential, and osteogenic functionality. (**B**) Representative footprints showing gait morphology, stride length, and force distribution. (**A**,**B**) Adapted from Ref. [98] under the terms of the Creative Commons Attribution License (CC BY). (**C**–**E**) In vivo evaluation of a SeNPs-incorporated LDH platform for osteosarcoma ablation and infected bone defect regeneration via multimodal imaging and morphological analysis. (**C**) A multifunctional SeNPs-incorporated MgFe-LDH nanosheets platform for a "one-stop-shop" strategy for postoperative osteosarcoma eradication with antibacterial and bone reconstruction. (**D**) Two-dimensional Micro-CT sagittal/coronal tomographic images (top row) and three-dimensional reconstruction images (bottom row) of a rabbit proximal tibia periprosthetic infection model after implantation of BGS, BGS@LDH, and BGS@LDH/Se scaffolds, used to assess periprosthetic bone destruction and osseointegration. (**E**) Gross image of the knee and surrounding tissues of osteosarcoma-bearing mice in BGS, BGS@LDH, and BGS@LDH/Se groups. (**C**–**E**) Adapted

from Ref. [14] under the terms of the Creative Commons Attribution License (CC BY). (**F**,**G**) Piezoelectric stimulation from TCP-PLA/GeSe scaffolds promotes nerve infiltration and revascularization for enhanced bone defect healing post-tumor resection. (**F**) Schematic illustration of the Piezoelectric biomimetic bone-periosteum scaffold (TCP-PLA/GeSe) for spatiotemporal innervated bone regeneration and tumor ablation. (**G**) 3D-reconstructed images of newly formed bone in different groups. (**F**,**G**) Adapted from Ref. [99] under the terms of the Creative Commons Attribution License (CC BY). (**H**,**I**) The selenium-doped calcium phosphate silicate nano-leaf coating (Se-CPS) on zinc-based implants improves osseointegration in infected bone defects through antibacterial and immunomodulatory effects. (**H**) Schematic of the fabrication process of the Se-CPS coating and its mechanism of promoting osteogenesis through antibacterial activity, xenophagy regulation, and macrophage immune polarization. (**I**) Micro-CT images of the medullary cavity and cancellous bone regions in rat tibiae 8 weeks after implantation of different samples (Ctrl, Zn, CPS, and Se-CPS) in a Staphylococcus aureus-infected model. (**H**,**I**) Adapted from Ref. [102] under the terms of the Creative Commons Attribution License (CC BY).

7.3. Se-Containing Biomaterials for the Treatment of Osteoarthritis

Osteoarthritis is a common degenerative joint disorder characterized by progressive articular cartilage deterioration and subchondral bone remodeling. The disease involves complex interactions between mechanical stress and biological responses in the joint. ECM degradation results from an imbalance between anabolic and catabolic activities in chondrocytes, leading to loss of tissue integrity and function [103]. A cross-sectional clinical survey reported that circulating Se concentrations were reduced by 9% and 7% in female patients with knee OA and concomitant knee-hip OA, respectively, compared with healthy controls. Although multivariate regression confirmed an independent observational association between lower serum Se status and OA after adjusting for age, BMI, and comorbidities, this female-specific cross-sectional study cannot establish whether reduced systemic Se is a causal driver or a secondary consequence of OA pathology [104].

Capitalizing on this critical biological link, Hu et al. engineered an injectable hydrogel using a dynamic Schiff base reaction between oxidized hyaluronic acid and hyaluronic acid-adipic acid dihydrazide for sustained SeNP delivery. The SeNP-laden hydrogel restored intracellular redox homeostasis and suppressed chondrocyte apoptosis in association with upregulated GPX1 expression and activity. Injected into the articular cavity of rats after DMM surgery, it reduced cartilage degeneration, inflammation-associated pain, and subchondral bone sclerosis [105]. To address the lack of targeting with conventional Se supplements, Liu et al. developed a cascade-targeted system (HA-SeNPs@AHAMA-HMs) by integrating hyaluronic acid-modified SeNPs into aldehyde-functionalized hydrogel microspheres. Hyaluronic acid binds CD44 receptors overexpressed on OA chondrocytes for precise targeting. In a DMM-induced rat OA model, this targeted microsphere system upregulated SEPHS1, a key regulator of redox homeostasis and selenoprotein expression in chondrocytes, thereby improving mitochondrial electron transport chain function and attenuating joint space narrowing and cartilage matrix degradation, demonstrating potential to slow OA progression (Figure 5A,B) [47].

Articular cartilage has no blood vessels, so OA treatments need to tackle two key issues: high oxidative stress in the joint cavity, and delivering regenerative signals deep into the cartilage matrix. Addressing this dual challenge, Gao et al. developed an injectable composite hydrogel crosslinked with SeNPs (Se/PRP-OGel) that co-encapsulates SeNPs and platelet-rich plasma (PRP) within an oxidized chondroitin sulfate-gelatin network. Comparative evaluations across blank hydrogel (OGel), SeNP-only hydrogel (Se-OGel), PRP-only hydrogel (PRP-OGel), and the combined Se/PRP-OGel platform demonstrated distinct incremental contributions: Se-OGel primarily scavenged ROS and mitigated joint inflammation, whereas PRP-OGel supplied sustained growth factors (such as

TGF-β and IGF) to stimulate ECM synthesis. In a rat OA model, the combined Se/PRP-OGel formulation achieved superior cartilage structural repair and subchondral bone preservation through these complementary functions (Figure 5C,D) [106].

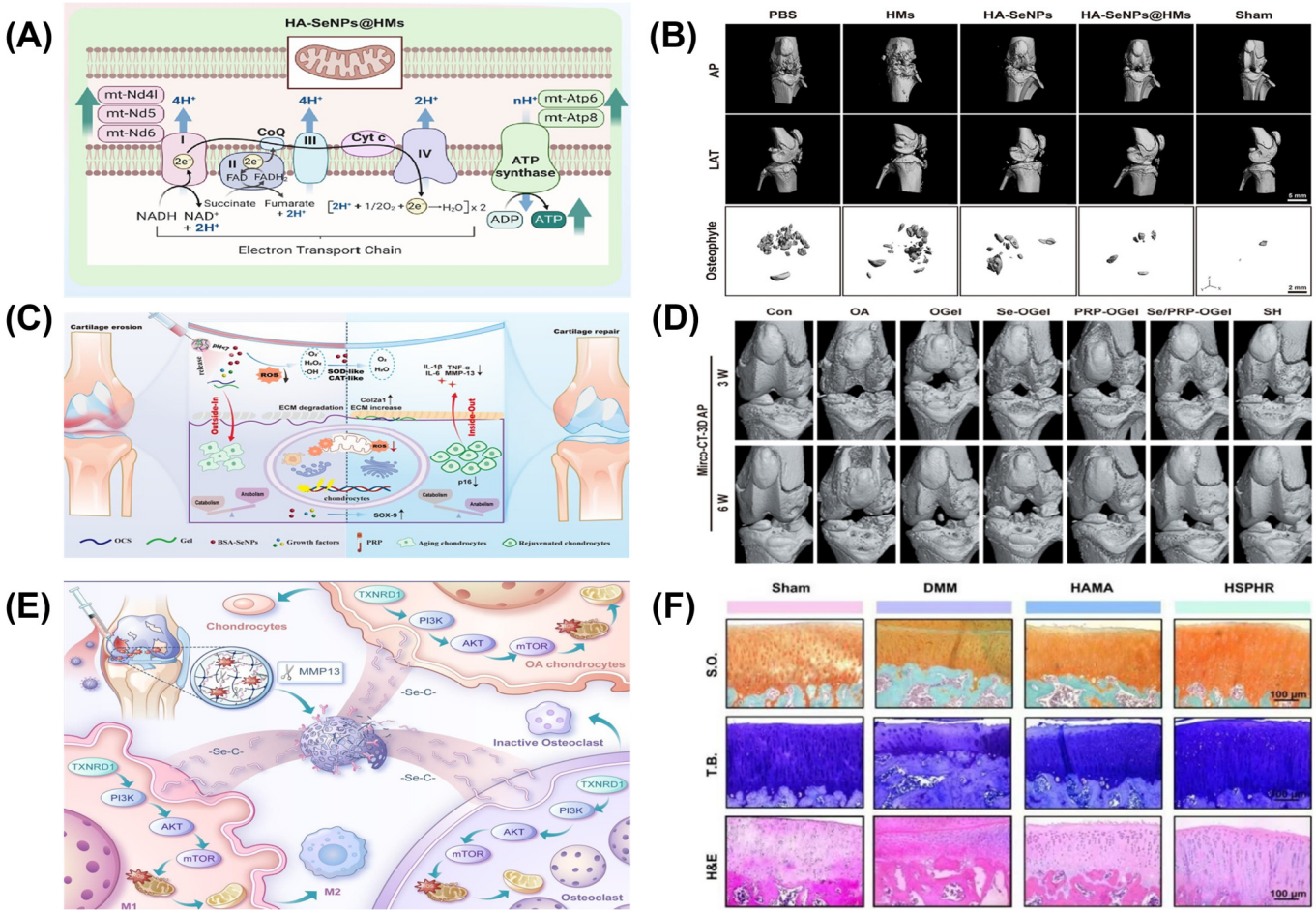

Figure 5. Selenium-containing biomaterials for osteoarthritis therapy. (**A**,**B**) Mechanism and in vivo evaluation of HA-SeNPs@AHAMA-HMs for osteoarthritis therapy. (**A**) After entering OA chondrocytes via cascade targeting, HA-SeNPs@AHAMA-HMs scavenge ROS and optimize mitochondrial electron transport chain function, thereby delaying OA progression. (**B**) 3D reconstruction images of the knee joints of SD rats in the Micro-CT experiment. (**A**,**B**) Reprinted with permission from Ref. [47]. License Number: 6311671316368. Copyright 2025, Elsevier. (**C**,**D**) From mechanism to structural restoration: Se/PRP-OGel hydrogel attenuates OA progression. (**C**) The mechanism of Se/PRP-OGel injectable hydrogel promoting cartilage regeneration in osteoarthritis. (**D**) Micro-CT imaging of knee joint structure at 3 and 6 weeks. (**C**,**D**) Reprinted with permission from Ref. [106]. License Number: 6311680137469. Copyright 2025, Elsevier. (**E**,**F**) Dual-responsive organic selenium delivery system enables multimodal osteoarthritis therapy. (**E**) The dual-response design delivers organic selenium to multiple joint tissues, enabling multimodal treatment for osteoarthritis. (**F**) Images of S.O., toluidine blue, hematoxylin, and eosin-stained sections of rat knee joint sections from different treatment subgroups. (**E**,**F**) Adapted from Ref. [107] under the terms of the Creative Commons Attribution License (CC BY).

Targeting the interplay between Fe^{2+} overload and lipid peroxidation in OA, Hu et al. engineered an injectable, self-healing composite hydrogel combining Fe^{2+}-capturing nanocatalysts with Se-enriched polypeptides releasing selenomethionine (SeMet). In this dual-component design, the nanocatalysts chelated excess labile Fe^{2+} to block Fenton-reaction-driven radical generation, while released SeMet served as an organic selenium donor that is metabolized into bioavailable selenocysteine precursors to support the biosynthesis and

activity of Sec-containing GPX4. Comparisons between individual components and the complete composite hydrogel in OA models showed that combining iron capture with SeMet delivery more effectively suppressed lipid peroxidation, restored chondrocyte mitochondrial homeostasis, and attenuated cartilage degeneration, accompanied by modulation of the PI3K/Akt/FOXO1 signaling axis [73].

Mitochondrial dysfunction is a core feature of OA, where impaired energy metabolism lowers ATP production and exacerbates M1/M2 macrophage imbalance. Liu et al. developed a dual ROS- and MMP13-responsive organic diselenide hydrogel microsphere system (HSPHR) via a thiol-ene click reaction. In preclinical OA models, HSPHR restored selenoprotein expression across cartilage, synovium, and subchondral bone, which was accompanied by elevated TXNRD1 levels and increased phosphorylation of the PI3K/Akt/mTOR pathway during cartilage repair, while simultaneously reducing monocyte oxidative stress to inhibit osteoclastogenesis and inflammatory macrophage polarization (Figure 5E,F) [107]. Taking a targeted biomolecular approach, Li et al. modified self-assembling nanoparticles with a cartilage-targeting peptide (WYRGRL) to co-deliver a diselenide-bridged diclofenac prodrug (DSeD) and the pro-chondrogenic small molecule kartogenin (KGN). Because blank DSeD nanoparticles, untargeted KGN@DSeD nanoparticles, and WYRGRL-targeted KGN@DSeD nanoparticles all share the DSeD prodrug backbone, comparisons across these three groups specifically isolated the incremental contributions of KGN loading and cartilage targeting: contrasting KGN@DSeD with blank DSeD nanoparticles demonstrated the pro-chondrogenic differentiation effect of KGN, whereas contrasting WYRGRL-KGN@DSeD with untargeted KGN@DSeD confirmed that the WYRGRL peptide prolonged intra-articular cartilage retention and further enhanced joint protection. Meanwhile, the properties of the shared diselenide-bridged DSeD backbone itself, namely ROS-triggered Se-Se bond cleavage, controlled diclofenac release, and associated NRF2 antioxidant pathway activation, were supported by separate in vitro H_2O_2-responsiveness and drug-release characterization alongside comparisons between blank DSeD nanoparticles and untreated OA controls. Together, these modules acted complementarily to preserve joint integrity in mouse OA models [45].

7.4. Se-Containing Biomaterials for Treating Intervertebral Disc (IVD) Degeneration

IVD degeneration is a common chronic musculoskeletal condition characterized by nucleus pulposus cell dysfunction, excessive ECM catabolism, and persistent oxidative stress. Current treatments with painkillers or physical therapy only relieve symptoms without halting structural deterioration, while surgical discectomy or spinal fusion disrupt native spinal biomechanics and increase adjacent segment degeneration risk [108].

Systemic Se supplementation or local Se delivery via biomaterial scaffolds enhances ROS scavenging and modulates inflammation in the avascular disc niche. Our laboratory previously showed that SeNPs protect nucleus pulposus cells from IL-1β-induced inflammation by activating GPX1 to restore mitochondrial integrity and redox balance. SeNPs increased matrix synthesis (aggrecan and type II collagen) while suppressing catabolic enzymes including MMP13 and ADAMTS. Local delivery in a rat puncture model preserved disc hydration and matrix deposition, mitigating IVD degeneration (Figure 6A,B) [109]. Se also ameliorates IVD degeneration by upregulating SELENOK to reduce ER stress, which suppresses aberrant intracellular calcium influx from excessive mechanical loading. Mechanotransduction through Piezo1 channels on plasma and ER membranes triggers ferroptosis under pathological strain. This dual mechanism restores redox homeostasis and stabilizes the IVD matrix (Figure 6C,D) [110].

The needle puncture model is the most widely used animal model for IVD degeneration, but it differs substantially from clinical surgical interventions [111]. In practice, discectomy relieves symptoms from herniated IVDs, but the residual nucleus pulposus

defect lacks effective regenerative solutions [112]. Our laboratory recently developed a Se-functionalized hydrogel microsphere system (SeNPs@GelMA) from gelatin methacrylate and SeNPs. SeNPs@GelMA microspheres alone provided only limited antioxidant microenvironment support, whereas significant reconstruction of nucleus pulposus extracellular matrix relied on the combined action of exogenous transplanted NPCs and selenium-containing microsphere carriers. Implantation of SeNPs@GelMA microspheres loaded with nucleus pulposus cells into rat caudal intervertebral discs after nucleotomy significantly promoted nucleus pulposus-like tissue regeneration and extracellular matrix deposition (e.g., aggrecan), effectively improving disc height (assessed by X-ray) and tissue hydration (assessed by MRI); however, direct recovery of biomechanical properties under load-bearing conditions still requires further mechanical testing (Figure 6E,F) [113].

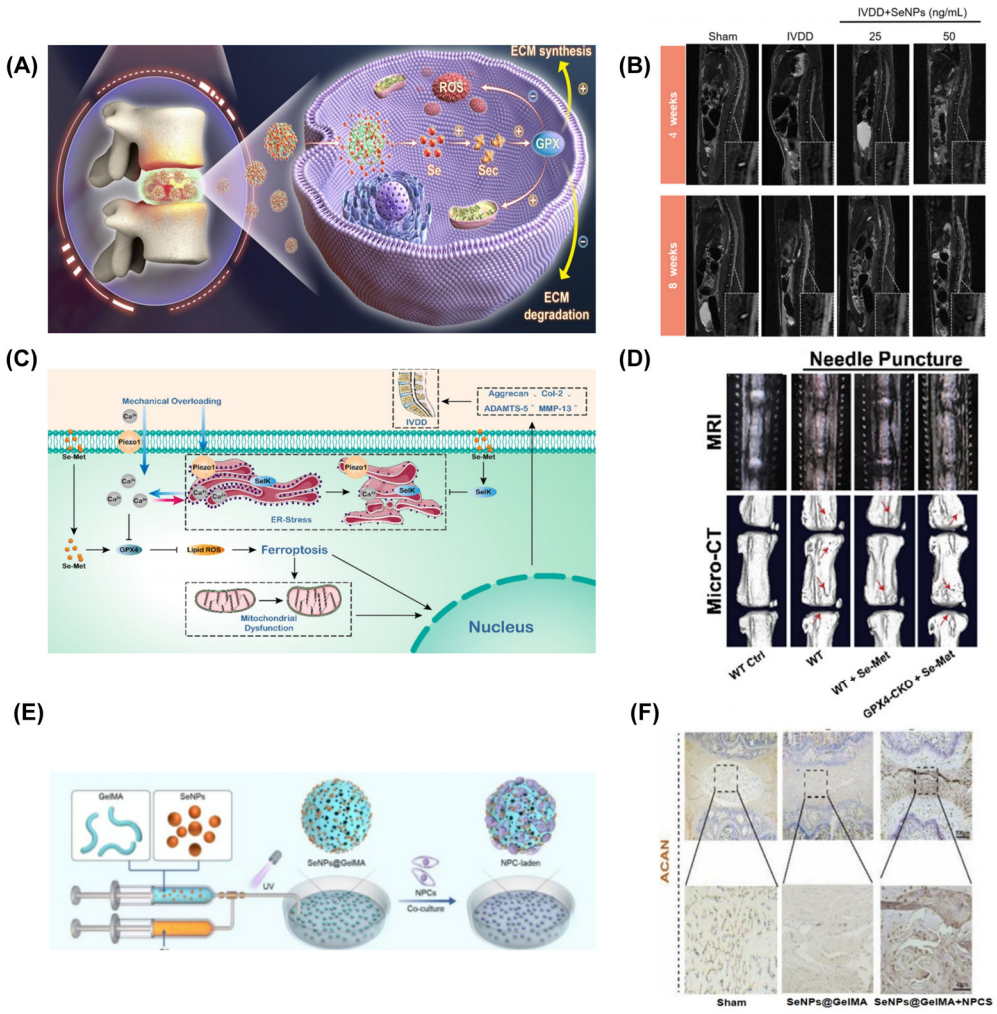

Figure 6. Selenium-containing biomaterials for intervertebral disc injury therapy. (**A**,**B**) Improved Pfirrmann grades and structural restoration in a rat IVDD model. (**A**) Schematic illustration of SeNPs ameliorating rat lumbar disc degeneration. SeNPs enhance expression of GPX1 and mitochondrial function of NPCs. (**B**) Representative sagittal T2-weighted MRI images and corresponding axial disc MRI insets (lower right corner) of the rat lumbar needle puncture degeneration model at weeks 4 and 8 after local treatment with different concentrations of SeNPs (25 and 50 ng/mL). (**A**,**B**) Adapted from Ref. [109] under the terms of the Creative Commons Attribution License (CC BY). (**C**,**D**) Se-Met inhibits ferroptosis to protect against disc degeneration. (**C**) Schematic diagram of how Selenium–SELENOK–GPX4 axis protects nucleus pulposus cells from mechanical overloading-induced ferroptosis. (**D**) The MRI and Micro-CT for coccygeal discs of mice. (**C**,**D**) Adapted from Ref. [110] under the terms of the Creative Commons Attribution License (CC BY). (**E**,**F**) NPC-laden

SeNPs@GelMA microspheres promote nucleus pulposus regeneration and restore intervertebral disc height after discectomy. (**E**) Schematic representation of NP tissue reconstruction using NPC-loaded SeNPs@GelMA microspheres. (**F**) Immunohistochemical staining for ACAN at the treatment site of the rat tail IVDs at 8 weeks post-surgery. (**E**,**F**) Reprinted with permission from Ref. [113]. License Number: 6311690853360. Copyright 2025, Elsevier.

7.5. Se-Containing Biomaterials for Treating Skeletal Muscle Diseases

Se controls skeletal myoblast differentiation through selenoproteins. These selenoproteins maintain redox balance and regulate key myogenic transcription factors. Sufficient Se availability supports myotube formation and maturation, and prevents oxidative stress from blocking the differentiation process. Investigating this dynamic at the cellular level, Lee et al. found that SeNPs reduce H_2O_2-induced oxidative damage in C2C12 myoblasts by inhibiting cell apoptosis and ROS accumulation. They also elevated the expression of myogenic regulators including MYOD, MYOG, ACTN, and MYH, accelerating myogenic maturation under oxidative stress (Figure 7A,B) [114].

Sarcopenia is a progressive condition in older adults. It causes rapid loss of skeletal muscle mass, strength, and physical ability. It is divided into two categories: primary decline linked to aging, and secondary forms caused by other factors. Secondary sarcopenia includes glucocorticoid-induced myopathy, muscle atrophy after sciatic nerve denervation, acute muscle damage from oxidative stress, and traumatic muscle volume loss [115].

Dietary or oral selenium supplementation alleviates glucocorticoid-induced skeletal muscle atrophy. In a mouse model of dexamethasone (Dex, intraperitoneal injection at 25 mg/kg)-induced muscle atrophy, oral gavage of sodium selenite (Na_2SeO_3) aqueous solution (20 μg/mL, 0.5 mL per dose, i.e., 10 μg/mouse, every other day for 3 weeks) significantly attenuated the decreases in body weight and grip strength and promoted recovery of gastrocnemius muscle mass. Additionally, this intervention increased the abundance of beneficial gut microbiota, particularly Lactobacillus and Dubosiella, suggesting a potential gut-muscle axis link (Figure 7C,D) [116]. However, traditional nutritional supplementation has clear limitations: poor bioavailability, side effects, and insufficient long-term effectiveness.

To overcome the pharmacokinetic limitations of free Se, Yu et al. developed leucine-loaded mesoporous silica nanoparticles bridged by diselenide bonds (Leu@Se-Se-MSNs). Comparative evaluations among free leucine, unloaded Se-Se-MSNs, and Leu@Se-Se-MSNs in dexamethasone- and denervation-induced sarcopenia models isolated their respective contributions: the Se-Se-MSN carrier underwent redox-responsive cleavage and metabolic conversion into selenocysteine to restore antioxidant selenoproteins and suppress Akt/FOXO3a/MuRF1-mediated proteolysis, whereas co-delivered leucine incrementally activated the mTOR/S6K axis to promote muscle protein synthesis. Thus, the overall anti-atrophy efficacy derived from the complementary actions of the diselenide nanocarrier and leucine [44]. Age-related decline in muscle strength is associated not only with loss of muscle mass but also with impaired sarcoplasmic reticulum (SR) calcium release and decreased endogenous selenoprotein N (SELENON) levels. Fodor et al. investigated the effects of dietary nano-selenium (NanoSe) supplementation (5 mg elemental Se/kg food, i.e., 5 ppm, administered for two months to untrained aged male mice) in comparison with a separate group of lifelong-trained aged mice. Both two-month dietary NanoSe supplementation in untrained aged mice and lifelong exercise training independently restored ex vivo twitch and tetanic contractile force, improved SR calcium release homeostasis, and upregulated SELENON protein expression in aged skeletal muscle compared with untrained aged controls, with NanoSe supplementation achieving functional improvements comparable to those observed in the lifelong-trained group. Mechanistically, neither NanoSe supplementation nor lifelong training reduced the age-related

protein degradation of ryanodine receptor 1 (RyR1); instead, the authors proposed that elevated SELENON expression and antioxidant capacity may improve excitation-contraction coupling by attenuating oxidative modification of the RyR1 channel [117].

Notably, because aqueous gavage concentrations (e.g., 20 μg/mL Na_2SeO_3 for 3 weeks) and dietary supplementation levels (e.g., 5 mg elemental Se/kg food for 2 months) involve distinct chemical species, vehicles, and exposure durations, they cannot be directly compared as equivalent systemic doses. When directly compared at matched oral selenium doses in adolescent rats, Nogales et al. observed divergent effects between selenite and SeNPs on skeletal muscle development: while SeNPs reduced oxidative stress, they impaired insulin-mTOR signaling and reduced muscle mass, shifting adolescent muscle metabolism toward catabolism, whereas selenite preserved muscle mass by maintaining an insulin-sensitive, pro-synthetic state [118].

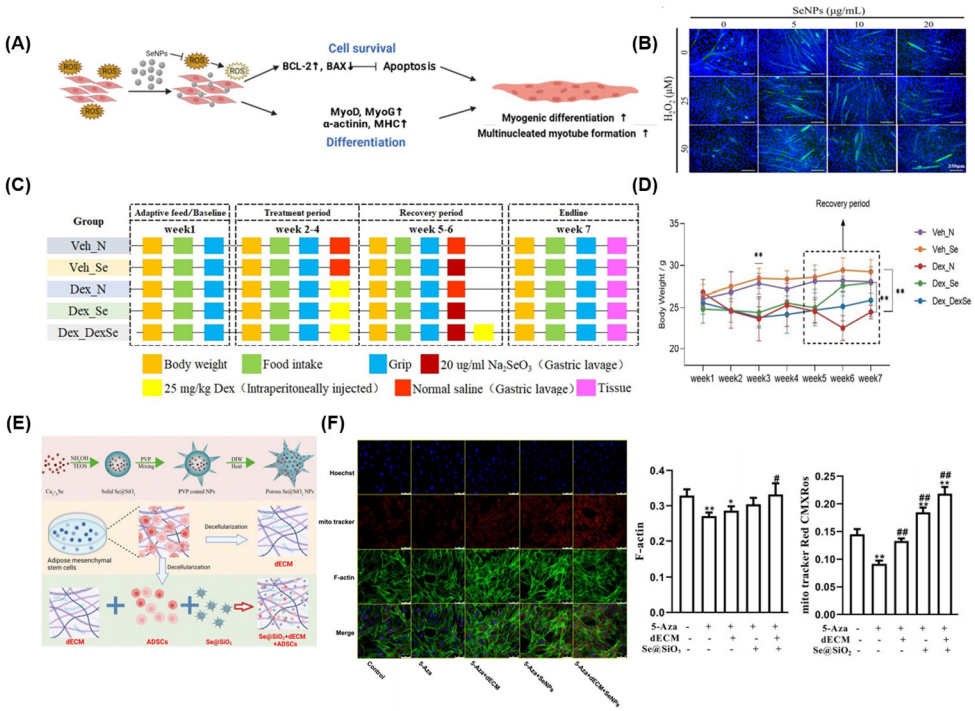

Figure 7. Application of selenium-containing biomaterials in the treatment of skeletal muscle injury. (**A**,**B**) SeNPs Promote Myogenic Differentiation of C2C12 Cells. (**A**) Schematic diagram of C2C12 cells cultured and treated with SeNPs for myogenic differentiation. (**B**) Image using MHC after 5 days of differentiation induced by SeNP treatment. (**A**,**B**) Adapted from Ref. [114] under the terms of the Creative Commons Attribution License (CC BY). (**C**,**D**) Oral sodium selenite supplementation alleviates dexamethasone (Dex)-induced skeletal muscle atrophy in mice. (**C**) Schematic of the in vivo experimental design and dosing timeline (week 1 acclimation; weeks 2–4 modeling/treatment; weeks 5–6 recovery; week 7 endpoint sampling), showing time points for body weight, food intake, grip strength, intraperitoneal Dex injection (25 mg/kg), and oral gavage of sodium selenite (20 μg/mL, 0.5 mL per dose). Five groups: Veh_N (control + saline gavage), Veh_Se (control + sodium selenite gavage), Dex_N (Dex model + saline gavage), Dex_Se (Dex for 3 weeks, then Dex discontinued and switched to sodium selenite gavage for recovery), and Dex_DexSe (continuous Dex modeling with concurrent sodium selenite gavage). (**D**) Body weight curves of the five groups from weeks 1 to 7 (dashed box indicates body weight differences during the recovery period, weeks 5–7). (**C**,**D**) Reprinted with permission from Ref. [116]. License Number: 1751502-1. Copyright 2024, RSC. (**E**,**F**) In vitro evaluation of porous Se@SiO_2 nanocomposites combined with dECM for promoting myogenic differentiation of ADSCs. (**E**) Schematic illustration of the preparation of porous Se@SiO_2 nanoparticles combined with ADSC-derived dECM and the in vitro 5-azacytidine (5-Aza)-induced

myogenic differentiation protocol. (**F**) Left: Representative fluorescence images of Hoechst (blue), Mito-Tracker (red), and F-actin (green) staining across treatment groups (Control, 5-Aza, 5-Aza + dECM, 5-Aza + Se@SiO_2, and 5-Aza + dECM + Se@SiO_2). Right: Quantitative analysis of F-actin fluorescence intensity and intracellular mitochondrial content (Mito-Tracker Red CMXRos), showing incremental improvements when dECM and porous Se@SiO_2 were applied together. (**E**,**F**) Adapted from Ref. [119] under the terms of the Creative Commons Attribution License (CC BY). * $p < 0.05$, ** $p < 0.01$ vs. control group. # $p < 0.05$, ## $p < 0.01$ vs. 5-Aza group.

Volumetric muscle loss (VML) is a severe condition in which traumatic avulsion or surgical resection exceeds the intrinsic regenerative capacity of skeletal muscle stem cells, often causing irreversible functional deficits and chronic disability. Zhang et al. engineered a porous Se@SiO_2 nanocomposite for sustained Se release and combined it with adipose-derived stem cell (ADSC)-derived decellularized ECM (dECM) to investigate their combined effects on the myogenic differentiation of ADSCs. In this composite system, the dECM scaffold provides a structural and biochemical niche, while the porous Se@SiO_2 nanoparticles scavenge excess intracellular ROS. In in vitro culture experiments, the combined application of dECM and porous Se@SiO_2 reduced cell apoptosis and ROS accumulation during 5-azacytidine induction, upregulated the expression of myogenic markers (MYOD, MYOG, DES, and MYH), and enhanced mitochondrial biogenesis and respiratory chain activity compared with either component alone (Figure 7E,F) [119]. Nevertheless, it must be emphasized that this study only provides in vitro cellular evidence of myogenic differentiation and mitochondrial protection, without evaluating tissue-level muscle regeneration or contractile force restoration in an in vivo VML animal defect model; thus, it represents an early in vitro proof-of-concept for future VML scaffold design. To clearly distinguish the study types, experimental models, delivery routes, measured endpoints, and primary limitations across epidemiological observations, systemic nutritional interventions, and localized biomaterial therapies in musculoskeletal disorders, representative studies are systematically summarized in Table 4.

Table 4. Compact evidence table: representative studies across musculoskeletal disease applications.

Disease/Application Area	Representative Study/Platform	Study Type	Species & Model	Administration Route	Key Endpoint Measures	Major Limitations	References
Bone health & osteoporosis	NHANES population study/meta-analysis	Population observational (cross-sectional/cohort)	Human adult cohorts	Dietary intake/serum Se baseline	Femoral BMD, FRAX risk estimates, self-reported fracture history	Observational association only; cannot establish causality; confounded by overall nutrition & lifestyle	[5,89]
Telomere-dysfunction bone aging	Dietary Se restriction model	Animal nutritional intervention	Short-telomere G3 $Terc^{-/-}$ knockout male mice	Systemic long-term dietary Se restriction vs. supplementation	Trabecular microarchitecture (Micro-CT), glucose tolerance, lifespan & premature aging phenotypes	Dependent on specific G3 $Terc^{-/-}$ genetic progeroid background; not generalizable to normal aging	[90]
Postmenopausal osteoporosis & bone defect	Se@SF/CPC cement/ASCDs carbon dots	Preclinical biomaterial intervention	OVX rats/mice with bone defect or systemic bone loss	Local implantation into distal femoral defect or intravenous targeted injection	Micro-CT BV/TV, histological mineralization, GPX1/GPX4 expression	Rodent bone remodeling differs from humans; lacks large-animal weight-bearing testing and long-term toxicokinetics	[13,91]

Infectious bone defect/osteomyelitis	Se-CPS coating on Zn implants	Preclinical biomaterial intervention	S. aureus-infected rat tibial osteomyelitis model	Intramedullary local implantation of coated Zn alloy prosthesis	Bacterial clearance, macrophage xenophagy & polarization, osseointegration Micro-CT, selenoprotein transcripts	Antibacterial & pro-osteogenic effects contributed by Zn ions, alkaline microenvironment, Ca/P/Si ions, and Se jointly; not Se alone	[102]
Osteoarthritis (OA)	Female knee/hip OA clinical survey	Population cross-sectional observational	Human female knee OA & knee-hip OA patients vs. controls	Serum trace element measurement	Circulating serum Se concentration vs. clinical OA diagnosis	Female-specific sample; cannot distinguish whether low Se is cause or consequence of OA	[104]
Osteoarthritis (OA)	HA-SeNPs@AHAMA-HMs/Se/PRP-OGel	Preclinical biomaterial intervention	Rat DMM-induced OA model	Intra-articular local injection	Joint space width, osteophyte formation (Micro-CT), cartilage matrix staining, SEPHS1/GPX1 expression	Rodent gait & cartilage thickness differ from humans; PRP growth factors and SeNPs jointly contribute to efficacy	[47,106]
Intervertebral disc degeneration (IVDD)	NPC-laden SeNPs@GelMA microspheres	Preclinical biomaterial + cell combined intervention	Rat coccygeal needle puncture or post-discectomy degeneration model	Intradiscal local microinjection	MRI hydration signal (Pfirrmann grade), X-ray disc height index, ACAN immunohistochemistry	Rat tail is non-weight-bearing; no direct ex vivo biomechanical compression test; efficacy includes transplanted NPC contribution	[113]
Sarcopenia/muscle atrophy (glucocorticoid & denervation)	Leu@Se-Se-MSNs	Preclinical biomaterial intervention	Mouse models of dexamethasone-induced and sciatic nerve denervation-induced muscle atrophy	Oral administration	Muscle mass, grip strength, myofiber cross-sectional area, selenoprotein expression, mTOR/S6K and Akt/FOXO3a/MuRF1 pathway markers	Efficacy reflects complementary actions of the diselenide-bridged MSN carrier and co-delivered leucine rather than Se alone	[44]
Glucocorticoid-induced muscle atrophy	Na_2SeO_3 aqueous oral gavage	Animal nutritional intervention	Mouse model of dexamethasone (25 mg/kg, i.p.)-induced skeletal muscle atrophy	Oral gavage (20 μg/mL Na_2SeO_3, 0.5 mL/dose, i.e., 10 μg/mouse, every other day for 3 weeks)	Body weight, grip strength, gastrocnemius muscle mass, gut microbiota profile (16S rRNA sequencing)	Narrow safety margin of inorganic selenite; gut-muscle axis association is correlative	[116]

Age-related skeletal muscle dysfunction	Dietary NanoSe supplementation vs. lifelong exercise training	Animal nutritional & exercise comparison	Untrained aged male mice (NanoSe-supplemented) vs. separate lifelong-trained aged mice and young/old controls	Dietary supplementation (5 mg elemental Se/kg food, i.e., 5 ppm NanoSe, for 2 months in untrained aged mice) vs. lifelong training	Ex vivo twitch and tetanic contractile force, SR Ca^{2+} release homeostasis, muscle SELENON and RyR1 protein levels	NanoSe and training were separate groups (not a combined intervention); RyR1 protein degradation was unchanged, and attenuated RyR1 oxidative modification was proposed as a mechanism rather than directly measured	[117]
Adolescent skeletal muscle development	Oral selenite vs. SeNPs comparison	Animal nutritional/nanomaterial comparison	Healthy adolescent male rats	Matched oral selenium doses of sodium selenite vs. SeNPs in diet/drinking water	Skeletal muscle mass, protein synthesis/degradation balance, GPX1 activity, insulin-mTOR signaling markers	Evaluated in healthy growing adolescent rats rather than a disease model; SeNPs impaired insulin-mTOR signaling and decreased muscle mass	[118]
Volumetric muscle loss (VML)	Se@SiO_2 + dECM composite	In vitro biomaterial scaffold development	ADSC myogenic differentiation (cell culture only)	In vitro scaffold culture; no in vivo VML model	MYOD/MYOG/DES/MYH expression, mitochondrial biogenesis & respiratory activity	In vitro proof-of-concept only; no animal VML model or functional muscle force testing	[119]

8. Future Perspectives

Selenium-containing biomaterials show clear therapeutic value for treating muscle and bone conditions. Even so, three real-world obstacles stop them from being widely used in clinics. First, selenium has a very narrow safe dosing range—too little does not work, and too much quickly becomes toxic, creating constant safety concerns. Second, the structural strength of the scaffolds does not line up with how fast they break down in the body, so they cannot both provide steady mechanical support for weight-bearing areas and release selenium at a controlled, even pace. Third, current manufacturing technology is not mature enough to make these materials at scale with consistent quality from batch to batch.

8.1. Biosafety, Pharmacokinetics, and the Narrow Therapeutic Window

Selenium is an essential trace element with a very narrow safety margin, meaning there is very little difference between an effective dose and a toxic dose. Different forms of selenium—selenite, selenomethionine, and SeNPs—follow distinct pathways of absorption, distribution, metabolism, and excretion in the body, which makes accurate dosing challenging [120]. Sustained-release microsphere systems adjust polymer molecular weight and breakdown rate to deliver selenium at a nearly steady rate, preventing dangerous concentration spikes from rapid burst release [121]. Cascade-targeted delivery relies on pH- or ROS-sensitive triggers in the inflammatory microenvironment to release selenium in a controlled, stepwise manner directly at the lesion site, keeping local therapeutic levels while lowering whole-body exposure [47]. Dynamic degradation control built on diselenide bonds aligns material breakdown with the pace of tissue repair

through redox-sensitive bond cleavage, so the drug is released exactly when and where it is needed.

8.2. Mechanical Integrity and Degradation Mismatch

Adding selenium often weakens the mechanical properties of polymer materials, which reduces how well scaffolds can deliver initial structural support and resist repeated stress in weight-bearing bone defects [122]. When organic and inorganic components of the scaffold degrade at different rates, it can also cause uneven breakdown of the structure or unexpected changes in selenium release patterns [123]. Future material development should combine structural improvements such as carbon fiber reinforcement, core–shell designs and gradient crosslinking networks with chemical approaches using reversible dynamic covalent bonds, so that degradation kinetics can be carefully and precisely adjusted.

8.3. Engineering Fabrication and Future Directions

Uniform composition, pore structure, selenium loading, and release behavior should be set as core quality standards. With this technology, selenium can be concentrated specifically in bone-inducing areas, while porosity and mechanical support can be adjusted separately [124]. Multi-component integration of selenium with other bioactive ions such as magnesium, strontium, or zinc in 3D-printed ceramic scaffolds combines the complementary functions of each element in osteogenesis, antibacterial activity, and oxidative stress regulation. This multi-component design is intended to avoid local cytotoxicity associated with high-dose use of a single element [14,102]. Although advanced manufacturing strategies such as 3D printing help improve the uniformity of scaffold pore structure and local selenium distribution, process optimization alone cannot directly resolve core barriers including long-term in vivo degradation toxicology, differences in systemic pharmacokinetics across different selenium chemical forms, and clinical safety verification.

9. Conclusions

Selenium-containing biomaterials represent promising preclinical intervention strategies for treating various complex musculoskeletal diseases. These platforms not only serve as trace element carriers but also regulate the pathological microenvironment through multiple mechanisms, including releasing bioavailable selenium to support the biosynthesis of endogenous Sec-containing selenoproteins, exerting the intrinsic GPX-mimicking nanozyme activity of the materials, enabling redox-responsive drug release via diselenide bonds, and cooperating with carriers and accompanying active components to remodel the immune-metabolic and cell differentiation microenvironment. Current preclinical studies, covering in vitro cell models and rodent models, have shown that these biomaterials effectively delay the progression of experimental osteoporosis and osteoarthritis, improve hydration and matrix deposition in degenerated or post-operative intervertebral discs, alleviate drug- or denervation-induced skeletal muscle atrophy, and demonstrate potential in supporting myogenic differentiation for developing scaffolds for volumetric muscle loss. However, it must be recognized that the current positive outcomes are mainly confined to the preclinical stage, and the efficacy of composite platforms often relies on the combined effects of selenium, carriers, and accompanying active components. Future clinical translation requires not only advanced manufacturing and dynamic chemical design to partially address mechanical mismatch and local burst release, but also rigorous validation of long-term biosafety, systemic pharmacokinetics, and direct biomechanical effects on tissues in large load-bearing animal models and clinical trials.

Author Contributions: Y.S.: Data curation, Formal analysis, Writing—original draft. X.D.: Data curation, Formal analysis, Writing—original draft. Y.Y.: Data curation, Formal analysis. F.H.: Conceptualization, Project administration, Supervision, Funding acquisition, Writing—review and editing. X.C.: Conceptualization, Supervision, Funding acquisition, Writing—review and editing. All authors have read and agreed to the published version of the manuscript.

Funding: This study was supported by the Changzhou Science and Technology Project (CJ20263089); Suzhou Applied Basic Research Programs (Health Care) of Science and Technology Innovation Projects (SYW2024069); the 14th Five-Year Plan High-Level Health Talents Training Project (2024CZBJ011); and the Key Laboratory of Orthopaedics of Suzhou (SZS2022017).

Institutional Review Board Statement: Not applicable.

Informed Consent Statement: Not applicable.

Data Availability Statement: No new data were created or analyzed in this study. Data sharing is not applicable to this article.

Acknowledgments: During the preparation of this manuscript, the authors used DeepSeek-V3 for the purposes of polishing textual expressions and refining wording. The authors have reviewed and edited the output and take full responsibility for the content of this publication.

Conflicts of Interest: The authors declare that the research was conducted in the absence of any commercial or financial relationships that could be construed as a potential conflict of interest.

Abbreviations

The following abbreviations are used in this manuscript:

ACTN	α-actinin
ADSCs	Adipose-derived stem cells
Akt	protein kinase B
ALP	alkaline phosphatase
ARG1	arginase 1
ATP	adenosine triphosphate
BGS	bioactive glass scaffold
BMD	bone mineral density
BMP2	bone morphogenetic protein 2
BTO	Barium Titanate
CMCSMA	Carboxymethyl chitosan methacryloyl
CSA	chondroitin sulfate A
dECM	decellularized extracellular matrix
DES	desmin
DIOs	iodothyronine deiodinases
DMM	destabilization of the medial meniscus
ECM	extracellular matrix
ER	endoplasmic reticulum
FAD	flavin adenine dinucleotide
Fe^{2+}	ferrous ion
FOXO1	forkhead box O1
FOXO3a	forkhead box O3
FRAX	Fracture Risk Assessment Tool
GelMA	methacrylated gelatin
GPXs	glutathione peroxidases
GR	glutathione reductase
GSH	glutathione
GSSG	oxidized GSH
H_2O_2	hydrogen peroxide
hMSCs	human mesenchymal stem cells

IGF	insulin-like growth factor
IL-1β	interleukin-1β
IL-6	interleukin-6
IL-8	interleukin-8
IVD	intervertebral disc
JNK	c-Jun N-terminal kinase
KBD	Kashin-Beck disease
LNT-Se	lentinan-modified surface-active SeNPs
MMP13	matrix metalloproteinase 13
MSDs	musculoskeletal diseases
mTOR	mammalian target of rapamycin
MuRF1	muscle RING finger 1
MYH	myosin heavy chain
Na_2SeO_3	Sodium selenite
NADPH	nicotinamide adenine dinucleotide phosphate
NFATc1	nuclear factor of activated T cells 1
NF-κB	nuclear factor kappa B
NPCs	nucleus pulposus cells
NRF2	nuclear factor erythroid 2-related factor 2
OA	osteoarthritis
OVX	ovariectomized
OXPHOS	oxidative phosphorylation
Pd	palladium
PDI	protein disulfide isomerase
PI3K	phosphoinositide 3-kinase
PLA	polylactic acid
PRDX	peroxiredoxin
PRP	platelet-rich plasma
RANKL	receptor activator of nuclear factor kappa B ligand
RONS	reactive oxygen and nitrogen species
ROS	reactive oxygen species
rT3	reverse triiodothyronine
RUNX2	runt-related transcription factor 2
RyR1	ryanodine receptor type 1
S6K	ribosomal protein S6 kinase signaling pathway
Se	selenium
Sec	selenocysteine
Sec-SeOH	selenenic acid
SELENON	selenoprotein N
SELENOW	selenoprotein W
SELENOK	selenoprotein K
Se-MBG	Se-doped mesoporous bioactive glass
SeMet	selenomethionine
SeNPs	selenium nanoparticles
SEPHS1	selenophosphate synthetase 1
SEPHS2	selenophosphate synthetase 2
SeYCQDs	Se-doped carbon quantum dots
SLC7A11	solute carrier family 7 member 11
SOX9	sex determining region Y-box 9
SP7 or Osterix	osteoblast-specific transcription factor (Sp7)
SR	sarcoplasmic reticulum
T2	diiodothyronine
T3	triiodothyronine
T4	thyroxine
TCA	tricarboxylic acid
TGF-β	transforming growth factor-beta
TNF-α	tumor necrosis factor-alpha
TXN	thioredoxin
TXNIP	thioredoxin-interacting protein

TXNRDs	thioredoxin reductases
VEGFA	vascular endothelial growth factor A
VML	volumetric muscle loss
ZIF-8	zeolitic imidazolate framework-8
β-TCP	β-tricalcium phosphate

References

1. Winther, K.H.; Rayman, M.P.; Bonnema, S.J.; Hegedüs, L. Selenium in thyroid disorders—Essential knowledge for clinicians. *Nat. Rev. Endocrinol.* **2020**, *16*, 165–176. https://doi.org/10.1038/s41574-019-0311-6.
2. Mousa, R.; Dardashti, R.N.; Metanis, N. Selenium and selenocysteine in protein chemistry. *Angew. Chem. Int. Ed. Engl.* **2017**, *56*, 15818–15827. https://doi.org/10.1002/anie.201706876.
3. Schweizer, U.; Fabiano, M. Genetics of selenoproteins and selenoprotein metabolism—An overview of current concepts and emerging aspects. *Redox Biol.* **2026**, *91*, 104083. https://doi.org/10.1016/j.redox.2026.104083.
4. Schomburg, L. Selenium, selenoproteins and the thyroid gland: Interactions in health and disease. *Nat. Rev. Endocrinol.* **2011**, *8*, 160–171. https://doi.org/10.1038/nrendo.2011.174.
5. Wu, C.C.; Wang, C.K.; Yang, A.M.; Lu, C.S.; Lin, C.Y. Selenium status is independently related to bone mineral density, FRAX score, and bone fracture history: NHANES, 2013 to 2014. *Bone* **2021**, *143*, 115631. https://doi.org/10.1016/j.bone.2020.115631.
6. Kang, D.; Lee, J.; Wu, C.; Guo, X.; Lee, B.J.; Chun, J.S.; Kim, J.H. The role of selenium metabolism and selenoproteins in cartilage homeostasis and arthropathies. *Exp. Mol. Med.* **2020**, *52*, 1198–1208. https://doi.org/10.1038/s12276-020-0408-y.
7. Dabravolski, S.A.; Sukhorukov, V.N.; Melnichenko, A.A.; Khotina, V.A.; Orekhov, A.N. The role of selenium in atherosclerosis development, progression, prevention and treatment. *Biomedicines* **2023**, *11*, 2010. https://doi.org/10.3390/biomedicines11072010.
8. Leszto, K.; Biskup, L.; Korona, K.; Marcinkowska, W.; Możdżan, M.; Węgiel, A.; Młynarska, E.; Rysz, J.; Franczyk, B. Selenium as a modulator of redox reactions in the prevention and treatment of cardiovascular diseases. *Antioxidants* **2024**, *13*, 688. https://doi.org/10.3390/antiox13060688.
9. Jehan, C.; Cartier, D.; Bucharles, C.; Anouar, Y.; Lihrmann, I. Emerging roles of ER-resident selenoproteins in brain physiology and physiopathology. *Redox Biol.* **2022**, *55*, 102412. https://doi.org/10.1016/j.redox.2022.102412.
10. Sabouri, Z.; Dequeecker, M.; Anees, H.; Adib, F.R.; Jamous, R.; Zheng, J.; Lyu, X.; Stoetzel, S.; Heiss, C.; El Khassawna, T.; et al. Recent advances in biomaterials for bone regeneration: Bridging innovation and clinical translation. *Mater. Today Bio* **2025**, *36*, 102685. https://doi.org/10.1016/j.mtbio.2025.102685.
11. Xu, H.; Cao, W.; Zhang, X. Selenium-containing polymers: Promising biomaterials for controlled release and enzyme mimics. *Acc. Chem. Res.* **2013**, *46*, 1647–1658. https://doi.org/10.1021/ar4000339.
12. Lu, H.H.; Ege, D.; Salehi, S.; Boccaccini, A.R. Ionic medicine: Exploiting metallic ions to stimulate skeletal muscle tissue regeneration. *Acta Biomater.* **2024**, *190*, 1–23. https://doi.org/10.1016/j.actbio.2024.10.033.
13. Zhou, Q.; Chen, W.; Gu, C.; Liu, H.; Hu, X.; Deng, L.; He, W.; Xu, Y.; Zhu, X.; Yang, H.; et al. Selenium-modified bone cement promotes osteoporotic bone defect repair in ovariectomized rats by restoring GPx1-mediated mitochondrial antioxidant functions. *Regen. Biomater.* **2023**, *10*, rbad011. https://doi.org/10.1093/rb/rbad011.
14. Bian, Y.; Zhao, K.; Hu, T.; Tan, C.; Liang, R.; Weng, X. A Se nanoparticle/MgFe-LDH composite nanosheet as a multifunctional platform for osteosarcoma eradication, antibacterial and bone reconstruction. *Adv. Sci.* **2024**, *11*, e2403791. https://doi.org/10.1002/advs.202403791.
15. Angelone, T.; Rocca, C.; Lionetti, V.; Penna, C.; Pagliaro, P. Expanding the frontiers of guardian antioxidant selenoproteins in cardiovascular pathophysiology. *Antioxid. Redox Signal.* **2024**, *40*, 369–432. https://doi.org/10.1089/ars.2023.0285.
16. Manful, C.F.; Fordjour, E.; Subramaniam, D.; Sey, A.A.; Abbey, L.; Thomas, R. Antioxidants and reactive oxygen species: Shaping human health and disease outcomes. *Int. J. Mol. Sci.* **2025**, *26*, 7520. https://doi.org/10.3390/ijms26157520.
17. Pitts, M.W.; Hoffmann, P.R. Endoplasmic reticulum-resident selenoproteins as regulators of calcium signaling and homeostasis. *Cell Calcium* **2017**, *70*, 76–86. https://doi.org/10.1016/j.ceca.2017.05.001.
18. Flohé, L.; Toppo, S.; Orian, L. The glutathione peroxidase family: Discoveries and mechanism. *Free Radic. Biol. Med.* **2022**, *187*, 113–122. https://doi.org/10.1016/j.freeradbiomed.2022.05.003.
19. Handy, D.E.; Loscalzo, J. The role of glutathione peroxidase-1 in health and disease. *Free Radic. Biol. Med.* **2022**, *188*, 146–161. https://doi.org/10.1016/j.freeradbiomed.2022.06.004.
20. Esworthy, R.S.; Doroshow, J.H.; Chu, F.F. The beginning of GPX2 and 30 years later. *Free Radic. Biol. Med.* **2022**, *188*, 419–433. https://doi.org/10.1016/j.freeradbiomed.2022.06.232.

21. Chang, C.; Worley, B.L.; Phaëton, R.; Hempel, N. Extracellular Glutathione Peroxidase GPx3 and Its Role in Cancer. *Cancers* **2020**, *12*, 2197. https://doi.org/10.3390/cancers12082197.
22. SharathBabu, B.N.; Shivangi, S.; Valiyaveettil, A.; Annaraj, B.; Mugesh, G. Small molecule selenium-based glutathione peroxidase 4 mimetic inhibits lipid peroxidation and protects cultured neurons from ferroptosis. *Free Radic. Biol. Med.* **2025**, *238*, 275–292. https://doi.org/10.1016/j.freeradbiomed.2025.06.047.
23. Brigelius-Flohé, R.; Flohé, L. Regulatory phenomena in the glutathione peroxidase superfamily. *Antioxid. Redox Signal.* **2020**, *33*, 498–516. https://doi.org/10.1089/ars.2019.7905.
24. Zhao, Y.; Xiao, D.; Zeng, M.; Gao, Y.; Huang, A.; Ren, C.; Du, Y. High glucose induces osteoblasts ferroptosis via the TXNIP/Trx-1/GPX4 pathway in type 2 diabetic osteoporosis. *Eur. J. Med. Res.* **2025**, *31*, 163. https://doi.org/10.1186/s40001-025-03749-z.
25. Reeves, M.A.; Hoffmann, P.R. The human selenoproteome: Recent insights into functions and regulation. *Cell. Mol. Life Sci.* **2009**, *66*, 2457–2478. https://doi.org/10.1007/s00018-009-0032-4.
26. Dou, Q.; Turanov, A.A.; Mariotti, M.; Hwang, J.Y.; Wang, H.; Lee, S.G.; Paulo, J.A.; Yim, S.H.; Gygi, S.P.; Chung, J.J.; et al. Selenoprotein TXNRD3 supports male fertility via the redox regulation of spermatogenesis. *J. Biol. Chem.* **2022**, *298*, 102183. https://doi.org/10.1016/j.jbc.2022.102183.
27. Köhrle, J.; Frädrich, C. Deiodinases control local cellular and systemic thyroid hormone availability. *Free Radic. Biol. Med.* **2022**, *193*, 59–79. https://doi.org/10.1016/j.freeradbiomed.2022.09.024.
28. Bianco, A.C.; Dumitrescu, A.; Gereben, B.; Ribeiro, M.O.; Fonseca, T.L.; Fernandes, G.W.; Bocco, B.M.L.C. Paradigms of Dynamic Control of Thyroid Hormone Signaling. *Endocr. Rev.* **2019**, *40*, 1000–1047. https://doi.org/10.1210/er.2018-00275.
29. Guo, H. Selenium-containing small molecules. *Commun. Chem.* **2022**, *5*, 138. https://doi.org/10.1038/s42004-022-00756-7.
30. Zeng, H.; Cao, J.J.; Combs, G.F. Selenium in bone health: Roles in antioxidant protection and cell proliferation. *Nutrients* **2013**, *5*, 97–110. https://doi.org/10.3390/nu5010097.
31. Ressler, A.; Antunović, M.; Cvetnić, M.; Ivanković, M.; Ivanković, H. Selenite substituted calcium phosphates: Preparation, characterization, and cytotoxic activity. *Materials* **2021**, *14*, 3436. https://doi.org/10.3390/ma14123436.
32. El-Saadony, M.T.; Saad, A.M.; Alkafaas, S.S.; Dladla, M.; Ghosh, S.; Mohammed, D.M.; Soliman, T.N.; Elkelish, A.; Khalil, F.M.A.; Fahmy, M.A.; et al. Selenium nanoparticles: Eco-friendly synthesis, biological activities and biomedical applications—A comprehensive review. *Mater. Today Bio* **2026**, *37*, 102946. https://doi.org/10.1016/j.mtbio.2026.102946.
33. Khurana, A.; Tekula, S.; Saifi, M.A.; Venkatesh, P.; Godugu, C. Therapeutic applications of selenium nanoparticles. *Biomed. Pharmacother.* **2019**, *111*, 802–812. https://doi.org/10.1016/j.biopha.2018.12.146.
34. Ferro, C.; Florindo, H.F.; Santos, H.A. Selenium nanoparticles for biomedical applications: From development and characterization to therapeutics. *Adv. Healthc. Mater.* **2021**, *10*, e2100598. https://doi.org/10.1002/adhm.202100598.
35. Chung, S.; Zhou, R.; Webster, T.J. Green synthesized BSA-coated selenium nanoparticles inhibit bacterial growth while promoting mammalian cell growth. *Int. J. Nanomed.* **2020**, *15*, 115–124. https://doi.org/10.2147/IJN.S193886.
36. Villaverde-Cantizano, G.; Laurenti, M.; Rubio-Retama, J.; Contreras-Cáceres, R. *Reducing Agents in Colloidal Nanoparticle Synthesis*; Mourdikoudis, S., Ed.; The Royal Society of Chemistry: London, UK, 2021; pp. 1–27. https://doi.org/10.1039/9781839163623-00001.
37. Geoffrion, L.D.; Hesabizadeh, T.; Medina-Cruz, D.; Kusper, M.; Taylor, P.; Vernet-Crua, A.; Chen, J.; Ajo, A.; Webster, T.J.; Guisbiers, G. Naked selenium nanoparticles for antibacterial and anticancer treatments. *ACS Omega* **2020**, *5*, 2660–2669. https://doi.org/10.1021/acsomega.9b03172.
38. Varlamova, E.G.; Turovsky, E.A.; Blinova, E.V. Therapeutic potential and main methods of obtaining selenium nanoparticles. *Int. J. Mol. Sci.* **2021**, *22*, 10808. https://doi.org/10.3390/ijms221910808.
39. Ishtiaq, S.; Hussain, G.; Zafar, H.K.; Liaquat, R.; Rasul, S.; Al-Kahtani, A.A.; Nafady, A.; Sohail, M. Facile synthesis of selenium nanoparticles for enhanced oxygen evolution reaction: Insights into electrochemical and photoelectrochemical catalysis. *ACS Omega* **2024**, *10*, 520–528. https://doi.org/10.1021/acsomega.4c07016.
40. He, L.; Zhang, Z.; Tang, Z.; Shen, K.; Sang, C.; Zheng, L.; Xiong, Z.; Chen, T. Industrial-level production of ultrastable selenium nanoparticles using a confined coordination synthetic strategy. *Cell Rep. Phys. Sci.* **2024**, *5*, 102303. https://doi.org/10.1016/j.xcrp.2024.102303.
41. Huang, S.W.; Yao, Y.Y.; Zhang, H.X.; Guo, W.Y.; Fang, M.H.; Wang, H.B.; Sun, Y.J.; Li, M.H. Novel mechanisms for selenite biotransformation and selenium nanoparticles biogenesis in *Acinetobacter sp. SX5* isolated from seleniferous soil. *J. Hazard. Mater.* **2025**, *489*, 137694. https://doi.org/10.1016/j.jhazmat.2025.137694.
42. Kim, G.M.; Oh, S.; Kim, K.S. Biogenic selenium nanoparticles from *Lactiplantibacillus plantarum* as a potent antimicrobial agent against methicillin-resistant Staphylococcus aureus. *Pharmaceutics* **2025**, *18*, 14. https://doi.org/10.3390/pharmaceutics18010014.

43. Tian, R.; Ma, H.; Ren, J.; Li, Y.; Zhang, Z.; Xu, Z.; He, L.; Zhu, C.; Xu, J.; Yu, S.; et al. Selenium-containing nanoscale hydrogen-bonded organic framework nanozymes for multienzyme cascade antioxidant-targeted therapy of cerebral ischemia-reperfusion injury. *ACS Nano* **2026**, *20*, 2435–2450. https://doi.org/10.1021/acsnano.5c20015.
44. Yu, Y.; Jiang, X.; Yu, T.; Chen, F.; Huang, R.; Xun, Z.; Wang, X.; Liu, X.; Xie, X.; Sun, C.; et al. Maintaining myoprotein and redox homeostasis via an orally recharged nanoparticulate supplement potentiates sarcopenia treatment. *Biomaterials* **2025**, *314*, 122863. https://doi.org/10.1016/j.biomaterials.2024.122863.
45. Li, Z.; Yuan, S.; Gong, C.; Qiao, L.; Wu, C.; Liu, Q.; Zhang, G.; Ai, Y.; Yang, W.; Chen, R.; et al. A diselenide-linkage self-assembled nanoprodrug for enhanced osteoarthritis treatment. *ACS Nano* **2025**, *19*, 40440–40455. https://doi.org/10.1021/acsnano.5c12637.
46. Moussa, Z.; Kaddoura, R.; Saadeh, H.A.; Abutaha, N.; Ahmed, S.A. Highly bioactive novel aryl-, benzyl-, and piperazine-selenoureas: Synthesis, structural characterization and in vitro biological evaluation. *Heliyon* **2022**, *8*, e10709. https://doi.org/10.1016/j.heliyon.2022.e10709.
47. Liu, J.; Liu, J.; Liu, S.; Xiao, P.; Du, C.; Zhan, J.; Chen, Z.; Chen, L.; Li, K.; Huang, W.; et al. Cascade targeting selenium nanoparticles-loaded hydrogel microspheres for multifaceted antioxidant defense in osteoarthritis. *Biomaterials* **2025**, *318*, 123195. https://doi.org/10.1016/j.biomaterials.2025.123195.
48. Bai, K.; Hong, B.; Huang, W.; He, J. Selenium-nanoparticles-loaded chitosan/chitooligosaccharide microparticles and their antioxidant potential: A chemical and in vivo investigation. *Pharmaceutics* **2020**, *12*, 43. https://doi.org/10.3390/pharmaceutics12010043.
49. Zhai, X.; Zhang, C.; Zhao, G.; Stoll, S.; Ren, F.; Leng, X. Antioxidant capacities of the selenium nanoparticles stabilized by chitosan. *J. Nanobiotechnol.* **2017**, *15*, 4. https://doi.org/10.1186/s12951-016-0243-4.
50. Ramachandran, T.; Manoharan, D.; Natesan, S.; Rajaram, S.K.; Karuppiah, P.; Shaik, M.R.; Khan, M.; Shaik, B. Synthesis and structural characterization of selenium nanoparticles-SP. MKUST-01 exopolysaccharide (SeNPs-EPS) conjugate for biomedical applications. *Biomedicines* **2023**, *11*, 2520. https://doi.org/10.3390/biomedicines11092520.
51. Hu, M.; Fang, J.; Zhang, Y.; Wang, X.; Zhong, W.; Zhou, Z. Design and evaluation a kind of functional biomaterial for bone tissue engineering: Selenium/mesoporous bioactive glass nanospheres. *J. Colloid Interface Sci.* **2020**, *579*, 654–666. https://doi.org/10.1016/j.jcis.2020.06.122.
52. Pantulap, U.; Arango-Ospina, M.; Boccaccini, A.R. Bioactive glasses incorporating less-common ions to improve biological and physical properties. *J. Mater. Sci. Mater. Med.* **2021**, *33*, 3. https://doi.org/10.1007/s10856-021-06626-3.
53. Swetha, R.; Priyangha, T. The synthesis and characterization of selenium-doped bioglass. *Cureus* **2024**, *16*, e61728. https://doi.org/10.7759/cureus.61728.
54. Laskus, A.; Zgadzaj, A.; Kolmas, J. Selenium-enriched brushite: A novel biomaterial for potential use in bone tissue engineering. *Int. J. Mol. Sci.* **2018**, *19*, 4042. https://doi.org/10.3390/ijms19124042.
55. Karahaliloğlu, Z.; Kilicay, E. In vitro evaluation of bone cements impregnated with selenium nanoparticles stabilized by phosphatidylcholine (PC) for application in bone. *J. Biomater. Appl.* **2020**, *35*, 385–404. https://doi.org/10.1177/0885328220933781.
56. Zhang, Z.; Zhang, J.; Xiao, J. Selenoproteins and selenium status in bone physiology and pathology. *Biochim. Biophys. Acta* **2014**, *1840*, 3246–3256. https://doi.org/10.1016/j.bbagen.2014.08.001.
57. Hou, J.; Tamura, Y.; Lu, H.Y.; Takahashi, Y.; Kasugai, S.; Nakata, H.; Kuroda, S. An in vitro evaluation of selenium nanoparticles on osteoblastic differentiation and antimicrobial properties against Porphyromonas gingivalis. *Nanomaterials* **2022**, *12*, 1850. https://doi.org/10.3390/nano12111850.
58. De Leon-Oliva, D.; Barrena-Blázquez, S.; Jiménez-Álvarez, L.; Fraile-Martinez, O.; García-Montero, C.; López-González, L.; Torres-Carranza, D.; García-Puente, L.M.; Carranza, S.T.; Álvarez-Mon, M.A.; et al. The RANK-RANKL-OPG system: A multifaceted regulator of homeostasis, immunity, and cancer. *Medicina* **2023**, *59*, 1752. https://doi.org/10.3390/medicina59101752.
59. Xie, Y.; Kang, R.; Klionsky, D.J.; Tang, D. GPX4 in cell death, autophagy, and disease. *Autophagy* **2023**, *19*, 2621–2638. https://doi.org/10.1080/15548627.2023.2218764.
60. Sharma, A.R.; Sharma, G.; Lee, Y.H.; Chakraborty, C.; Lee, S.S.; Seo, E.M. Sodium selenite promotes osteoblast differentiation via the WNT/β-catenin signaling pathway. *Cell J.* **2022**, *24*, 309–315. https://doi.org/10.22074/cellj.2022.8314.
61. Sahin, E.; Arafat, M.; Koparal, A.T. Selenomethionine, a trace element, increases osteoblastic activity of hFOB 1.19 cells (an in vitro study). *Biol. Trace Elem. Res.* **2024**, *202*, 5000–5005. https://doi.org/10.1007/s12011-023-04055-7.
62. Fatima, S.; Alfrayh, R.; Alrashed, M.; Alsobaie, S.; Ahmad, R.; Mahmood, A. Selenium nanoparticles by moderating oxidative stress promote differentiation of mesenchymal stem cells to osteoblasts. *Int. J. Nanomed.* **2021**, *16*, 331–343. https://doi.org/10.2147/IJN.S285233.

63. Wu, Z.; Hou, Q.; Qin, L.; Chen, T.; Yang, K.; Wei, F.; Wang, L. GPx-mimetic selenium-enriched yeast nanozymes ameliorate diabetic bone disease via dual-targeting of ROS scavenging and angiogenesis-osteogenesis coupling. *Mater. Today Bio* **2025**, *32*, 101836. https://doi.org/10.1016/j.mtbio.2025.101836.
64. Zou, B.; Xiong, Z.; Yu, Y.; Shi, S.; Li, X.; Chen, T. Rapid selenoprotein activation by selenium nanoparticles suppresses osteoclastogenesis and pathological bone loss. *Adv. Mater.* **2024**, *36*, e2401620. https://doi.org/10.1002/adma.202401620.
65. Zhang, L.; Wu, X.; Feng, Y.; Zheng, L.; Jian, J. Selenium donors inhibit osteoclastogenesis through inhibiting IL-6 and plays a pivotal role in bone metastasis from breast cancer. *Toxicol. Res.* **2020**, *9*, 544–551. https://doi.org/10.1093/toxres/tfaa053.
66. Zou, B.; Xiong, Z.; He, L.; Chen, T. Reversing breast cancer bone metastasis by metal organic framework-capped nanotherapeutics via suppressing osteoclastogenesis. *Biomaterials* **2022**, *285*, 121549. https://doi.org/10.1016/j.biomaterials.2022.121549.
67. Kim, H.; Lee, K.; Kim, J.M.; Kim, M.Y.; Kim, J.R.; Lee, H.W.; Chung, Y.W.; Shin, H.I.; Kim, T.; Park, E.S.; et al. Selenoprotein W ensures physiological bone remodeling by preventing hyperactivity of osteoclasts. *Nat. Commun.* **2021**, *12*, 2258. https://doi.org/10.1038/s41467-021-22565-7.
68. Liu, L.; Luo, P.; Wen, P.; Xu, P. Effects of selenium and iodine on Kashin-Beck disease: An updated review. *Front. Nutr.* **2024**, *11*, 1402559. https://doi.org/10.3389/fnut.2024.1402559.
69. Wang, X.; Jin, Z.; Chen, M.; Duan, D.; Lammi, M.J.; Guo, X.; Chang, Y. Inhibiting the aberrant activation of Wnt/β-catenin signaling by selenium supplementation ameliorates deoxynivalenol-induced toxicity and catabolism in chondrocytes. *J. Cell. Physiol.* **2020**, *235*, 4434–4442. https://doi.org/10.1002/jcp.29319.
70. Han, J.; Deng, H.; Li, Y.; Qiao, L.; Jia, H.; Zhang, L.; Wang, L.; Qu, C. Nano-elemental selenium particle developed via supramolecular self-assembly of chondroitin sulfate A and Na_2SeO_3 to repair cartilage lesions. *Carbohydr. Polym.* **2023**, *316*, 121047. https://doi.org/10.1016/j.carbpol.2023.121047.
71. Deng, H.; Deng, F.; Wen, X.; Jiang, Y.; Amhare, A.F.; Qiao, L.; Li, M.; Wan, P.; Wang, J.; Han, J. Targets and potential mechanism of chondroitin sulfate a-selenium nanoparticle on Kashin-Beck disease chondrocytes. *Biol. Trace Elem. Res.* **2025**, *203*, 5537–5552. https://doi.org/10.1007/s12011-025-04584-3.
72. Hu, J.; Luo, P.; Zhang, W.; Chen, T.; Yang, X.; Chen, Z.; Huang, S.; Zhang, X.; Kuang, Z.; Zhang, B. Phycocyanin-functionalized selenium nanoparticles attenuate osteoarthritis through ferroptosis suppression and modulation of the MAPK pathway. *Mater. Today Bio* **2026**, *38*, 103113. https://doi.org/10.1016/j.mtbio.2026.103113.
73. Hu, W.; Kang, F.; Li, Y.; Xu, Y.; Li, X.; Zhang, J.; Liao, J.; Dai, J.; Gong, X.; Li, J.; et al. An attack and defense strategy for osteoarthritis repair: Constructing a trace element modulated hydrogel to mitigate ferroptosis and promote cartilage matrix reconstruction. *Research* **2025**, *8*, 0979. https://doi.org/10.34133/research.0979.
74. Yan, J.; Guo, Y.; Fei, Y.; Zhang, R.; Han, Y.; Lu, S. GPx1 knockdown suppresses chondrogenic differentiation of ATDC5 cells through induction of reductive stress. *Acta Biochim. Biophys. Sin.* **2017**, *49*, 110–118. https://doi.org/10.1093/abbs/gmw125.
75. Xu, X.M.; Carlson, B.A.; Irons, R.; Mix, H.; Zhong, N.; Gladyshev, V.N.; Hatfield, D.L. Selenophosphate synthetase 2 is essential for selenoprotein biosynthesis. *Biochem. J.* **2007**, *404*, 115–120. https://doi.org/10.1042/BJ20070165.
76. Kang, D.; Lee, J.; Jung, J.; Carlson, B.A.; Chang, M.J.; Chang, C.B.; Kang, S.B.; Lee, B.C.; Gladyshev, V.N.; Hatfield, D.L.; et al. Selenophosphate synthetase 1 deficiency exacerbates osteoarthritis by dysregulating redox homeostasis. *Nat. Commun.* **2022**, *13*, 779. https://doi.org/10.1038/s41467-022-28385-7.
77. Choi, B.; Lee, C.; Yu, J.W. Distinctive role of inflammation in tissue repair and regeneration. *Arch. Pharm. Res.* **2023**, *46*, 78–89. https://doi.org/10.1007/s12272-023-01428-3.
78. Al-Mubarak, A.A.; Mavrogenis, G.M.; Guo, X.; de Bruyn, M.; Nath, M.; Romaine, S.P.R.; Beverborg, N.G.; Gomez, K.A.; Zijlstra, S.N.; van Veldhuisen, D.J.; et al. Biomarker and transcriptomics profiles of serum selenium concentrations in patients with heart failure are associated with immunoregulatory processes. *Redox Biol.* **2024**, *70*, 103046. https://doi.org/10.1016/j.redox.2024.103046.
79. Brüne, B.; Dehne, N.; Grossmann, N.; Jung, M.; Namgaladze, D.; Schmid, T.; von Knethen, A.; Weigert, A. Redox control of inflammation in macrophages. *Antioxid. Redox Signal.* **2013**, *19*, 595–637. https://doi.org/10.1089/ars.2012.4785.
80. Li, J.; Zhang, L.; Peng, J.; Zhao, C.; Li, W.; Yu, Y.; Huang, X.; Yang, F.; Deng, X.; Yang, X.; et al. Mitochondrial metabolic regulation of macrophage polarization in osteomyelitis and other orthopedic disorders: Mechanisms and therapeutic opportunities. *Front. Cell Dev. Biol.* **2025**, *13*, 1604320. https://doi.org/10.3389/fcell.2025.1604320.
81. Divakaruni, A.S.; Hsieh, W.Y.; Minarrieta, L.; Duong, T.N.; Kim, K.K.O.; Desousa, B.R.; Andreyev, A.Y.; Bowman, C.E.; Caradonna, K.; Dranka, B.P.; et al. Etomoxir inhibits macrophage polarization by disrupting CoA homeostasis. *Cell Metab.* **2018**, *28*, 490–503.e7. https://doi.org/10.1016/j.cmet.2018.06.001.

82. Chen, D.; Liang, Z.; Su, Z.; Huang, J.; Pi, Y.; Ouyang, Y.; Luo, T.; Guo, L. Selenium-doped mesoporous bioactive glass regulates macrophage metabolism and polarization by scavenging ROS and promotes bone regeneration. *ACS Appl. Mater. Interfaces* **2023**, *15*, 34378–34396. https://doi.org/10.1021/acsami.3c03446.
83. Chen, X.; Yang, Y.; Chen, J.; He, Y.; Huang, Y.; Huang, Q.; Deng, W.; Zhu, R.; Huang, X.; Li, T. Dual-driven selenium Janus single-atom nanomotors for autonomous regulating mitochondrial oxygen imbalance to catalytic therapy of rheumatoid arthritis. *Redox Biol.* **2025**, *81*, 103574. https://doi.org/10.1016/j.redox.2025.103574.
84. Korwar, A.M.; Hossain, A.; Lee, T.J.; Shay, A.E.; Basrur, V.; Conlon, K.; Smith, P.B.; Carlson, B.A.; Salis, H.M.; Patterson, A.D.; et al. Selenium-dependent metabolic reprogramming during inflammation and resolution. *J. Biol. Chem.* **2021**, *296*, 100410. https://doi.org/10.1016/j.jbc.2021.100410.
85. Misra, S.; Lee, T.J.; Sebastian, A.; McGuigan, J.; Liao, C.; Koo, I.; Patterson, A.D.; Rossi, R.M.; Hall, M.A.; Albert, I.; et al. Loss of selenoprotein W in murine macrophages alters the hierarchy of selenoprotein expression, redox tone, and mitochondrial functions during inflammation. *Redox Biol.* **2023**, *59*, 102571. https://doi.org/10.1016/j.redox.2022.102571.
86. Ouyang, J.; Deng, B.; Zou, B.; Li, Y.; Bu, Q.; Tian, Y.; Chen, M.; Chen, W.; Kong, N.; Chen, T.; et al. Oral hydrogel microbeads-mediated in situ synthesis of selenoproteins for regulating intestinal immunity and microbiota. *J. Am. Chem. Soc.* **2023**, *145*, 12193–12205. https://doi.org/10.1021/jacs.3c02179.
87. Cai, J.; Hu, J.; Zhang, Z.; Ma, S.; Dou, H.; Pan, D.; Geng, B.; Li, P.; Shen, L. Immunomodulatory carbon dots balance the anti-inflammatory, antibacterial, and osteogenic activities of metal-phenolic network for osteomyelitis therapy. *Biomaterials* **2026**, *334*, 124313. https://doi.org/10.1016/j.biomaterials.2026.124313.
88. Chandran, M.; Thiyagarajan, J.A.; Alokail, M.; Bruyère, O.; Harvey, N.C.; Rizzoli, R.; Veronese, N.; Reginster, J.Y. WHO benchmarks for equitable hip-fracture care and osteoporosis treatment in older people. *Nat. Rev. Rheumatol.* **2026**, *22*, 62–70. https://doi.org/10.1038/s41584-025-01319-5.
89. Xie, H.; Wang, N.; He, H.; Yang, Z.; Wu, J.; Yang, T.; Wang, Y. The association between selenium and bone health: A meta-analysis. *Bone Jt. Res.* **2023**, *12*, 423–432. https://doi.org/10.1302/2046-3758.127.BJR-2022-0420.R1.
90. Wu, R.T.; Cao, L.; Mattson, E.; Witwer, K.W.; Cao, J.; Zeng, H.; He, X.; Combs, G.F.; Cheng, W.H. Opposing impacts on health-span and longevity by limiting dietary selenium in telomere dysfunctional mice. *Aging Cell* **2017**, *16*, 125–135. https://doi.org/10.1111/acel.12529.
91. Cao, J.; Dong, Q.; Du, K.; Zhang, M.; Chen, W.; Hou, Z. Bone-targeting selenium-doped carbon dot-based nanoparticles for ferroptosis suppression and osteogenesis against postmenopausal osteoporosis. *Adv. Healthc. Mater.* **2026**, *15*, e05203. https://doi.org/10.1002/adhm.202505203.
92. Gorter, E.A.; Reinders, C.R.; Krijnen, P.; Appelman-Dijkstra, N.M.; Schipper, I.B. The effect of osteoporosis and its treatment on fracture healing: A systematic review of animal and clinical studies. *Bone Rep.* **2021**, *15*, 101117. https://doi.org/10.1016/j.bonr.2021.101117.
93. Huang, L.; Zhang, S.; Bian, M.; Xiang, X.; Xiao, L.; Wang, J.; Lu, S.; Chen, W.; Zhang, C.; Mo, G.; et al. Injectable, anti-collapse, adhesive, plastic and bioactive bone graft substitute promotes bone regeneration by moderating oxidative stress in osteoporotic bone defect. *Acta Biomater.* **2024**, *180*, 82–103. https://doi.org/10.1016/j.actbio.2024.04.016.
94. Rosslenbroich, S.B.; Oh, C.W.; Kern, T.; Mukhopadhaya, J.; Raschke, M.J.; Kneser, U.; Krettek, C. Current management of diaphyseal long bone defects—A multidisciplinary and international perspective. *J. Clin. Med.* **2023**, *12*, 6283. https://doi.org/10.3390/jcm12196283.
95. Shanmugavadivu, A.; Lekhavadhani, S.; Miranda, P.J.; Selvamurugun, N. Current approaches in tissue engineering-based nanotherapeutics for osteosarcoma treatment. *Biomed. Mater.* **2024**, *19*, 022003. https://doi.org/10.1088/1748-605X/ad270b.
96. He, Z.; Mu, Y.Q.; Gao, W.D.; Liu, Y.; Liu, S.B.; Liu, H.H.; Xing, J.W.; Han, W.J.; Miao, G.H.; Luo, E.; et al. Inflammatory cytokine scavenging and macrophage metabolism reprogramming to orchestrate inflammatory bone regeneration. *Mater. Horiz.* **2026**, *13*, 6601–6620. https://doi.org/10.1039/d6mh00561f.
97. Zou, X.; Fan, X.; Xu, P.; Yu, X.; Luo, C.; Kang, Z.; Shen, X.; Zheng, J.; Wang, J.; He, B.; et al. Selenium-albumin corona rinse ameliorates diabetic periodontitis by inhibiting inflammation, anti-bacterial and improving osteogenesis via activating TrxR1/ROS/β-catenin anti-oxidation cascade. *Biomaterials* **2026**, *328*, 123835. https://doi.org/10.1016/j.biomaterials.2025.123835.
98. Jiang, S.; Cai, B.; Ye, C.; Wu, K.; Liu, K.; Xu, P.; Liu, F.; Liu, Y. Immunomodulatory hydrogel coating with SeNPs and lithium silicate synergistically promotes osseointegration and prevents infection on titanium implants. *Adv. Sci.* **2026**, *13*, e13195. https://doi.org/10.1002/advs.202513195.

99. Xu, Y.; Xu, C.; Song, H.; Feng, X.; Ma, L.; Zhang, X.; Li, G.; Mu, C.; Tan, L.; Zhang, Z.; et al. Biomimetic bone-periosteum scaffold for spatiotemporal regulated innervated bone regeneration and therapy of osteosarcoma. *J. Nanobiotechnol.* **2024**, *22*, 250. https://doi.org/10.1186/s12951-024-02430-7.
100. Croes, M.; van der Wal, B.C.H.; Vogely, H.C. Impact of bacterial infections on osteogenesis: Evidence from in vivo studies. *J. Orthop. Res.* **2019**, *37*, 2067–2076. https://doi.org/10.1002/jor.24422.
101. Lei, C.; Lei, J.; Zhang, X.; Wang, H.; He, Y.; Zhang, W.; Tong, B.; Yang, C.; Feng, X. Heterostructured piezocatalytic nanoparticles with enhanced ultrasound response for efficient repair of infectious bone defects. *Acta Biomater.* **2023**, *172*, 343–354. https://doi.org/10.1016/j.actbio.2023.10.006.
102. Mao, M.; Chen, J.; Zhao, L.; Li, Q.; Liu, X.; Liu, Y.; Zhang, L. Regulating xenophagy and phenotype of macrophages by selenium-doped nanoleaves on Zn-based implants for infected bone integration. *Bioact. Mater.* **2026**, *63*, 868–884. https://doi.org/10.1016/j.bioactmat.2026.04.022.
103. Collins, K.H.; Haugen, I.K.; Neogi, T.; Guilak, F. Osteoarthritis as a systemic disease. *Nat. Rev. Rheumatol.* **2026**, *22*, 105–117. https://doi.org/10.1038/s41584-025-01332-8.
104. Skalny, A.V.; Menshikova, I.V.; Korobeinikova, T.V.; Morozova, G.D.; Guo, X.; Zhang, F.; Tinkov, A. Circulating essential trace element and mineral levels in female patients with knee or concomitant knee and hip osteoarthritis. *Biol. Trace Elem. Res.* **2026**, *204*, 568–579. https://doi.org/10.1007/s12011-025-04696-w.
105. Hu, W.; Yao, X.; Li, Y.; Li, J.; Zhang, J.; Zou, Z.; Kang, F.; Dong, S. Injectable hydrogel with selenium nanoparticles delivery for sustained glutathione peroxidase activation and enhanced osteoarthritis therapeutics. *Mater. Today Bio* **2023**, *23*, 100864. https://doi.org/10.1016/j.mtbio.2023.100864.
106. Gao, W.; Li, S.; Miao, Y.; Yuan, G.; Li, G.; Zhou, G.; Jia, G.; Yang, X.; Jin, Y. Selenium nanozyme-crosslinked composite hydrogel for promoting cartilage regeneration in osteoarthritis via an integrated 'outside-in' and 'inside-out' strategy. *J. Colloid Interface Sci.* **2025**, *693*, 137612. https://doi.org/10.1016/j.jcis.2025.137612.
107. Liu, Y.; Zhang, Y.; Yu, C.; Xia, X.; Kang, K.; Wu, Y.; Deng, Y.; Yu, J.; Hou, M.; Luo, Z.; et al. Organic di-selenide hydrogel microspheres for multimodal treatment of osteoarthritis. *Nat. Commun.* **2026**, *17*, 2300. https://doi.org/10.1038/s41467-026-68817-2.
108. Hammoor, B.T.; Lai, C.S.; Xiong, G.X.; Elliott, D.M.; Snyder, B.; Vresilovic, E.; Bono, C.M.; Freedman, B.R. Intervertebral disc degeneration. *Nat. Rev. Dis. Primers* **2026**, *12*, 5. https://doi.org/10.1038/s41572-025-00681-8.
109. He, W.; Tian, X.; Zhou, Q.; Lv, J.; Li, Y.; Jin, C.; Liu, H.; Yang, H.; Xu, Y.; He, F.; et al. Selenium nanoparticles ameliorate lumbar disc degeneration by restoring GPX1-mediated redox homeostasis and mitochondrial function of nucleus pulposus cells. *J. Nanobiotechnol.* **2024**, *22*, 634. https://doi.org/10.1186/s12951-024-02890-x.
110. Jia, C.; Xiang, Z.; Zhang, P.; Liu, L.; Zhu, X.; Yu, R.; Liu, Z.; Wang, S.; Liu, K.; Wang, Z.; et al. Selenium-SelK-GPX4 axis protects nucleus pulposus cells against mechanical overloading-induced ferroptosis and attenuates senescence of intervertebral disc. *Cell. Mol. Life Sci.* **2024**, *81*, 49. https://doi.org/10.1007/s00018-023-05067-1.
111. Ambrosio, L.; Vadalà, G.; di Rinaldis, E.; Muthu, S.; Ćorluka, S.; Buser, Z.; Meisel, H.J.; Yoon, S.T.; Denaro, V. Discectomy versus sequestrectomy in the treatment of lumbar disc herniation: A systematic review and meta-analysis. *Spine J.* **2025**, *25*, 211–226. https://doi.org/10.1016/j.spinee.2024.09.007.
112. Shi, L.; Jiang, L.; Xing, T.; Liu, K.; Chen, C.; Ma, P.; Winkler, T.; Qin, A.; Zhao, J. Cell-based therapies for intervertebral disc degeneration: Navigating the path from promise to clinical reality. *J. Orthop. Transl.* **2026**, *56*, 101041. https://doi.org/10.1016/j.jot.2025.101041.
113. Lv, J.; Shen, Y.; Zhou, Q.; He, W.; Chen, Y.; Chen, X.; Yang, H.; Xu, Y.; He, F.; Liu, T. Selenium-functionalized hydrogel microspheres promote nucleus pulposus reconstruction by activating selenoprotein-mediated mitochondrial redox homeostasis and energy metabolism. *Biomaterials* **2026**, *328*, 123826. https://doi.org/10.1016/j.biomaterials.2025.123826.
114. Lee, S.C.; Lee, N.H.; Patel, K.D.; Jun, S.K.; Park, J.H.; Knowles, J.C.; Kim, H.W.; Lee, H.H.; Lee, J.H. A study on myogenesis by regulation of reactive oxygen species and cytotoxic activity by selenium nanoparticles. *Antioxidants* **2021**, *10*, 1727. https://doi.org/10.3390/antiox10111727.
115. Mao, X.; Lv, K.; Qi, W.; Cheng, W.; Li, T.; Sun, Y.; Jin, H.; Pan, H.; Wang, D. Research progress on sarcopenia in the musculoskeletal system. *Bone Res.* **2025**, *13*, 78. https://doi.org/10.1038/s41413-025-00455-8.
116. Cheng, Y.; Liu, X.; Hao, Y.; Wang, S.; Wu, F.; Zhao, L.; Peng, D.; Du, Y.; Sheng, S.; Li, J.; et al. Selenium-mediated alleviation of skeletal muscle atrophy through enterotype modulation in mice. *Food Funct.* **2024**, *15*, 11619–11629. https://doi.org/10.1039/d4fo03889d.

117. Fodor, J.; Al-Gaadi, D.; Czirják, T.; Oláh, T.; Dienes, B.; Csernoch, L.; Szentesi, P. Improved calcium homeostasis and force by selenium treatment and training in aged mouse skeletal muscle. *Sci. Rep.* **2020**, *10*, 1707. https://doi.org/10.1038/s41598-020-58500-x.
118. Nogales, F.; Pajuelo, E.; Gallego-López, M.D.C.; Romero-Herrera, I.; Merchán, F.; Carreras, O.; Ojeda, M.L. Dissimilar effects of selenite and selenium nanoparticles on skeletal muscle development unrelated to GPx1 activity during adolescence in rats. *Nutrients* **2025**, *17*, 1841. https://doi.org/10.3390/nu17111841.
119. Zhang, Y.C.; Yang, Y.X.; Liu, Y.; Liu, X.J.; Dai, J.H.; Gao, R.S.; Hu, Y.Y.; Fei, W.Y. Combining porous Se@SiO nanocomposites and dECM enhances the myogenic differentiation of adipose-derived stem cell. *Int. J. Nanomed.* **2023**, *18*, 7661–7676. https://doi.org/10.2147/IJN.S436081.
120. Ringuet, M.T.; Hunne, B.; Lenz, M.; Bravo, D.M.; Furness, J.B. Analysis of bioavailability and induction of glutathione peroxidase by dietary nanoelemental, organic and inorganic selenium. *Nutrients* **2021**, *13*, 1073. https://doi.org/10.3390/nu13041073.
121. Cavalu, S.; Prokisch, J.; Laslo, V.; Vicas, S. Preparation, structural characterisation and release study of novel hybrid microspheres entrapping nanoselenium, produced by green synthesis. *IET Nanobiotechnol.* **2017**, *11*, 426–432. https://doi.org/10.1049/iet-nbt.2016.0107.
122. Karakuzu-İkizler, B.; Terzioğlu, P.; Oduncu-Tekerek, B.S. Effect of selenium incorporation on the structure and in vitro bioactivity of 45S5 bioglass. *J. Aust. Ceram. Soc.* **2020**, *56*, 697–709. https://doi.org/10.1007/s41779-019-00388-6.
123. Sowjanya, V.; Manuel, J.; Prasad, A.; Sasikanth, P.; Rao, P.V.; Madaboosi, N.; Veeraiah, N.; Prasad, P.S. Multifunctional role of selenium in biomaterials: Recent advances in synthesis, properties, and biomedical applications. *J. Alloys Compd.* **2025**, *1047*, 184978. https://doi.org/10.1016/j.jallcom.2025.184978.
124. Vaquette, C.; Bock, N.; Tran, P. Layered antimicrobial selenium nanoparticle-calcium phosphate coating on 3D printed scaffolds enhanced bone formation in critical size defects. *ACS Appl. Mater. Interfaces* **2020**, *12*, 55638–55648. https://doi.org/10.1021/acsami.0c17017.

Disclaimer/Publisher's Note: The statements, opinions and data contained in all publications are solely those of the individual author(s) and contributor(s) and not of MDPI and/or the editor(s). MDPI and/or the editor(s) disclaim responsibility for any injury to people or property resulting from any ideas, methods, instructions or products referred to in the content.